



2010-11-19

Proteoliposome Proton Flux Assays Establish Net Conductance, pH-Sensitivity, and Functional Integrity of a Novel Truncate of the M2 Ion "Channel" of Influenza A

Emily Peterson

Brigham Young University - Provo

Follow this and additional works at: <https://scholarsarchive.byu.edu/etd>

 Part of the [Cell and Developmental Biology Commons](#), and the [Physiology Commons](#)

BYU ScholarsArchive Citation

Peterson, Emily, "Proteoliposome Proton Flux Assays Establish Net Conductance, pH-Sensitivity, and Functional Integrity of a Novel Truncate of the M2 Ion "Channel" of Influenza A" (2010). *All Theses and Dissertations*. 2420.
<https://scholarsarchive.byu.edu/etd/2420>

This Thesis is brought to you for free and open access by BYU ScholarsArchive. It has been accepted for inclusion in All Theses and Dissertations by an authorized administrator of BYU ScholarsArchive. For more information, please contact scholarsarchive@byu.edu, ellen_amatangelo@byu.edu.

Proteoliposome Proton Flux Assays Establish Net Conductance, pH-
Sensitivity, and Functional Integrity of a Novel Truncate
of the M2 Ion “Channel” of Influenza A

Emily Peterson

A thesis submitted to the faculty of
Brigham Young University
in partial fulfillment of the requirements for the degree of
Master of Science

David D. Busath, Chair
Dixon J. Woodbury
Sterling N. Sudweeks
F. Brent Johnson

Department of Physiology and Developmental Biology
Brigham Young University
December 2010

Copyright © 2010 Emily Peterson
All Rights Reserved

BRIGHAM YOUNG UNIVERSITY

SIGNATURE PAGE

of a thesis submitted by

Emily Peterson

The thesis of Emily Peterson is acceptable in its final form including (1) its format, citations, and bibliographical style are consistent and acceptable and fulfill university and department style requirements; (2) its illustrative materials including figures, tables, and charts are in place; and (3) the final manuscript is satisfactory and ready for submission.

Date

David D. Busath, Chair

Date

Dixon J. Woodbury

Date

Sterling N. Sudweeks

Date

F. Brent Johnson

Date

Graduate Coordinator

Date

Dean, College of Life Sciences

ABSTRACT

Proteoliposome Proton Flux Assays Establish Net Conductance, pH-Sensitivity, and Functional Integrity of a Novel Truncate of the M2 Ion “Channel” of Influenza A

Emily Peterson

Department of Physiology and Developmental Biology

Master of Science

A novel truncate of Influenza A M2 protein (residues 22-62), incorporated into a uniquely tailored proteoliposome proton uptake assay, demonstrated proton flux more characteristic of an ion transporter than a traditional ion “channel.” The liposome paradigm was essential for testing the conductance activity of this M2 truncate at a range of extraphysiological pHs appropriate for channel vs. transport function determination. In addition to transporter-typical proton flux, M2(22-62) showed the key characteristics of functional integrity: selective proton uptake into liposomes and block of uptake by amantadine. Two sets of proteoliposome proton flux assays were carried out, Set 1 at pH values of 6.5, 6.0, 5.5, 5.0, and 4.5; Set 2 at pH values of 6.25, 6.0, 5.75, 5.5, 5.25, 5.0, and 4.75. Observed flux rates followed a proton transport saturation curve similar to that observed in mouse erythroleukemia cells¹. Proton transport was maximal at pH 5.5 in Set 1 (139 H⁺/second/tetramer) and at pH 5.75 in Set 2 (43 H⁺/second/tetramer). Amantadine block was strongest at pH 5.5 in Set 1 and 6.25 in Set 2, and apparent desensitization of the protein severely reduced proton flux and amantadine sensitivity below pH 5.5 in both sets of experiments. Decreased external pH increased proton uptake with an apparent pK_a of 6 (Set 1) or 6.5 (Set 2). These data indicate acid activation of M2(22-62) between pH 5.5-6, optimal amantadine block between pH 5.5-6.25, and a loss of peptide functionality between pH 5.9-4.7.

Keywords: Influenza A, M2 protein, proton transporter, proton channel, acid activation, proteoliposome, liposome, amantadine

ACKNOWLEDGMENTS

Thanks to: Mukesh Sharma and Timothy A. Cross of Florida State University Department of Chemistry and Biochemistry and National High Magnetic Field Laboratory, for providing the purified M2(22-62) protein truncate. Rafal M. Pielak and James J. Chou, of Harvard University, and Sindra P. Årsköld, of Lund University, for assistance in development and/or refinement of the liposome assay. Dixon J. Woodbury also assisted with assay considerations, and was also instrumental in creation of the Microsoft Excel data analysis method. Ted Ryser gathered and analyzed data to quantify liposomal depolarization rates, and Spencer Funk gathered and analyzed data relating to optimum protein:lipid ratios for proton flux assay measurements. Ted Ryser, Dan Inouye, Spencer Funk, Doug Bretzing, and Rachel Debenham all assisted occasionally with proton flux assay materials preparation. Thanks to my committee: Dixon J. Woodbury, Sterling N. Sudweeks, and F. Brent Johnson, for intellectual and material support, mentorship, and encouragement. And finally, my committee chair, David D. Busath, who provided inspiration for this project, background expertise on M2, assistance (when needed) with most aspects of data collection and analysis, effort to prepare and submit data for publication, and encouragement at all stages of the project.

Table of Contents

| | |
|---|-----------|
| INTRODUCTION..... | 1 |
| JUSTIFICATION FOR RESEARCH..... | 1 |
| <i>Figure 1.</i> | 4 |
| <i>Figure 2.</i> | 5 |
| EXPERIMENTAL DESIGN..... | 7 |
| LIPOSOME ASSAY INTRODUCTION | 7 |
| <i>Figure 3.</i> | 9 |
| PROTEOLIPOSOME COMPOSITION/PREPARATION | 10 |
| PROTON FLUX ASSAY DESIGN AND EXECUTION | 13 |
| <i>Figure 4.</i> | 15 |
| DATA EXTRACTION..... | 17 |
| <i>Figure 5.</i> | 18 |
| ANALYSIS..... | 19 |
| <i>Figure 6.</i> | 20 |
| RESULTS..... | 21 |
| PROTON FLUX, ACID-ACTIVATION, AND AMANTADINE BLOCK QUANTITATION | 21 |
| <i>Figure 7.</i> | 21 |
| <i>Figure 8.</i> | 22 |
| <i>Figure 9.</i> | 24 |
| <i>Figure 10.</i> | 25 |
| <i>Figure 11.</i> | 26 |
| FACTORS TO CONSIDER WHEN INTERPRETING RESULTS | 26 |
| <i>Figure 12.</i> | 27 |
| DISCUSSION..... | 30 |
| FUNCTIONAL CHARACTERISTICS OF M2(22-62) | 30 |
| <i>Figure 13.</i> | 32 |
| <i>Figure 14.</i> | 33 |
| <i>Figure 15.</i> | 35 |
| <i>Figure 16.</i> | 36 |
| APPENDIX..... | 39 |
| OPTIMAL LIPOSOME PROTEIN DENSITY DETERMINATION..... | 39 |
| <i>Figure 17.</i> | 39 |
| LIPOSOMAL LIPID QUANTITATION/VERIFICATION..... | 40 |
| LIPOSOMAL PROTEIN QUANTITATION ATTEMPTS..... | 41 |
| REFERENCES..... | 43 |
| WORKS CITED | 43 |
| CURRICULUM VITAE | 45 |
| EMILY PETERSON | 45 |

Proteoliposome Proton Flux Assays Establish Net Conductance, pH-Sensitivity, and Functional Integrity of a Novel Truncate of the M2 Ion “Channel” of Influenza A

INTRODUCTION

Justification for Research

Influenza A M2 is a 97-residue, homotetrameric integral membrane protein that forms a H⁺-selective pore in cell compartment membranes. The initial function of this proton conductance is to lower the pH inside the viral capsid, dissociating the genome and ribonucleoproteins from each other. Later, when nascent virions are assembled and awaiting release in membranous “envelopes” from the cell, M2 regulates the pH inside *trans*-Golgi vesicles to stabilize viral envelope proteins such as pH-sensitive hemagglutinin².

The M2 protein is the target of the anti-influenza adamantane-derived drugs amantadine and rimantadine. Amantadine has been in wide use since the 1970s³, and in the last few years (since about 2002) almost all emerging strains of influenza—including the most recent pandemic H1N1 strain⁴--have been shown to contain mutations in the M2 gene that confer viral resistance to these drugs.

This recent development in the fight against a very threatening human disease--as well as a desire to enhance knowledge and understanding of ion channel structure and function—has led myself and fellow investigators to consider the M2 protein a critically important subject of research. Some of the most key structural and functional characteristics of this protein are still unsettled in the field. For example, what is the exact rate of proton movement through the protein? Estimates have varied from 20/second in proteoliposome studies⁵ to 3000/second in

Xenopus oocytes⁶. How does amantadine block M2, and why are various mutants resistant to the drug? This question must rely heavily on structural studies such as x-ray crystallography and NMR, but functional assays are critical in verifying the integrity of protein mutants, truncates, and synthesized peptides thus tested. And finally, what is the mechanism of proton flux? Is M2 a traditional transmembrane “channel,” with ion passage limited only by concentration and electrical gradients across the membrane? Or is it more of a “transporter,” with a maximum rate of H⁺ transport limited by integral structural features of the protein, no matter how strong the driving forces on either side of the membrane^{7,8}?

In order to study M2-mediated ion flux across membranes, researchers have used a small variety of both *in vitro* and *in vivo* electrophysiological techniques: protein-induced flux measured by electrical current flow across a planar bilayer⁸; two-electrode voltage clamping of M2-expressing mouse erythroleukemia cells, CK-1 cells, or *Xenopus laevis* oocytes^{1,2,5,6}; or measurement of pH change inside or outside an M2 proteoliposome suspension^{3,4,7}.

Four distinctive characteristics of M2 activity have been well established in oocytes^{6,9-12} and mammalian cells^{1,13,14}: proton selectivity^{6,10,12}, acid activation¹¹, amantadine sensitivity¹⁵, and basic block of proton backflux^{8,11}. These characteristics are used as markers of protein function and integrity in M2 studies done now in any *in vivo* or *in vitro* system. Proton flux data from voltage-clamped MEL cells have also shown that H⁺ conductance through M2 reaches saturation at pH 4.0, with an apparent pK of 6.0¹. One of the primary aims of this thesis research was to provide additional conductance studies (in liposomes) to help determine whether this fifth property, structurally-determined maximal (“saturated”) H⁺ flux with a pK of ~6, can be included in the list of characteristic M2 behaviors.

Cultured cell or oocyte experiments are useful for providing an *in vivo* study method that eliminates uncertainties about correct protein synthesis, processing, and folding, as well as questions regarding membrane composition and proper protein insertion/orientation within the membrane. However, an entire oocyte plasmalemma can contain M2 tetramers by the billion, and even patch clamping a relatively small section of the membrane still yields a section with huge numbers of ion channels—and not all of the membrane proteins will be M2. Furthermore, quantitation of tetramers within the plasmalemma is restricted mainly to imprecise immunoblotting methods, leaving the per-channel flux calculations dependent on possible over- or underestimates of active M2 protein in the membrane.

Planar bilayers provide a method for precisely controlling solution/ion composition on either side of the membrane, membrane lipid species ratios, bilayer thickness, and density of inserted protein (from an expression system such as transfected *E.coli* or SF9 cells). However, problems arise from the surface strain due to suspension, and possibly from the planar shape of these artificial bilayers. Previous planar bilayer studies with M2 yielded high conductance and no amantadine block, seeming to indicate unusual protein configurations or aggregation, possibly as a consequence of the lateral pull exerted by the abnormal tautness and flatness of the bilayer¹⁶.

The most natural *in vitro* system in which to study M2 function is the proteoliposome^{2,4,7}. This method combines the precise control over protein-lipid ratio, lipid composition, and bath solution components gained by a planar bilayer assay, with the advantages of unstrained, spontaneously-formed lipid-protein spheres similar in size to an actual Influenza virus¹⁷. The liposome assay is more effective than *Xenopus* oocyte assays when using truncated M2 peptides, yet provides equally robust data^{18,19}. Liposomes can also withstand a much broader pH range than what is physiologically tolerable for cell or tissue culture models. For these reasons,

proteoliposome assays were chosen as the experimental paradigm in this effort to determine maximum single-channel flux rates through M2.

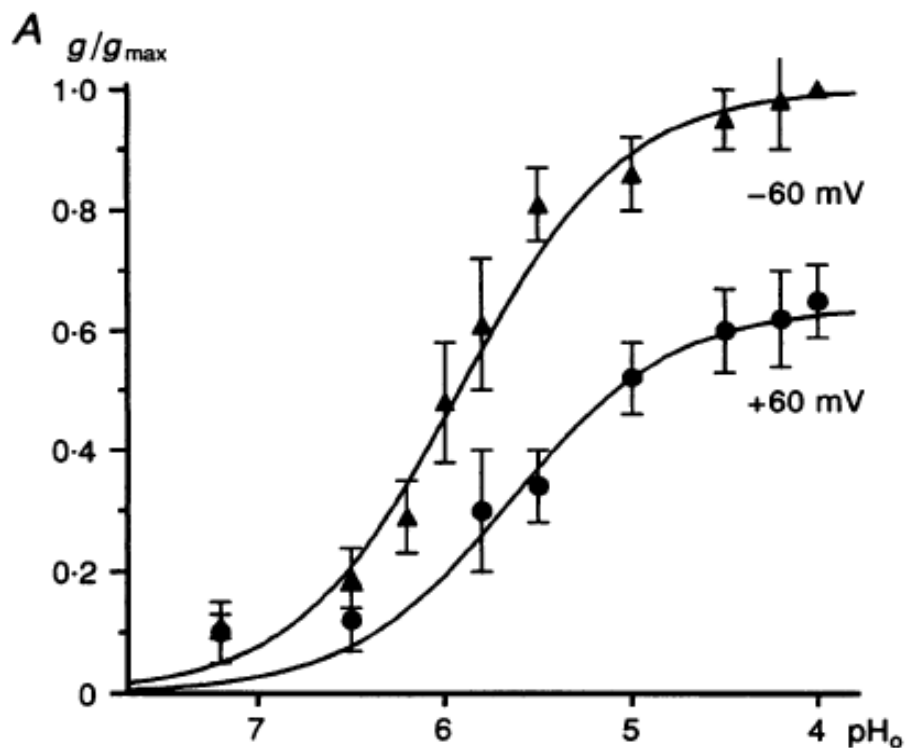


Figure 1.

Whole-cell voltage clamp of M2-transformed mouse erythroleukemia cells, from Chizhnikov, et. al¹. Legend in original publication: “Effect of pH_o on M2 conductance. A, chord conductance $g=I_H/(V-E_H)$ normalized to pH_o 4 at -60 mV plotted against pH_o at -60 and +60 mV; pH_i 7.4. Single site binding function was fitted by least-squares regression with a K_p of 1.2 μ M at -60 mV and 2.3 μ M at +60 mV.”

Investigators using whole-cell clamp measurement of M2-induced proton flux into mouse erythroleukemia cells obtained the single-site binding curve in Figure 1, suggesting transporter-like H⁺ flux function in M2, rather than channel-like proton passage. But no researchers have yet examined this suggestion by testing M2-induced proton flux in liposomes using a stepwise array of pH values. This approach can be optimally used with the liposome system, rather than live

cells, and is capable of determining whether M2 functions on a more subtly pH-dependent proton passage continuum, rather than simply being “active” or “inactive.”

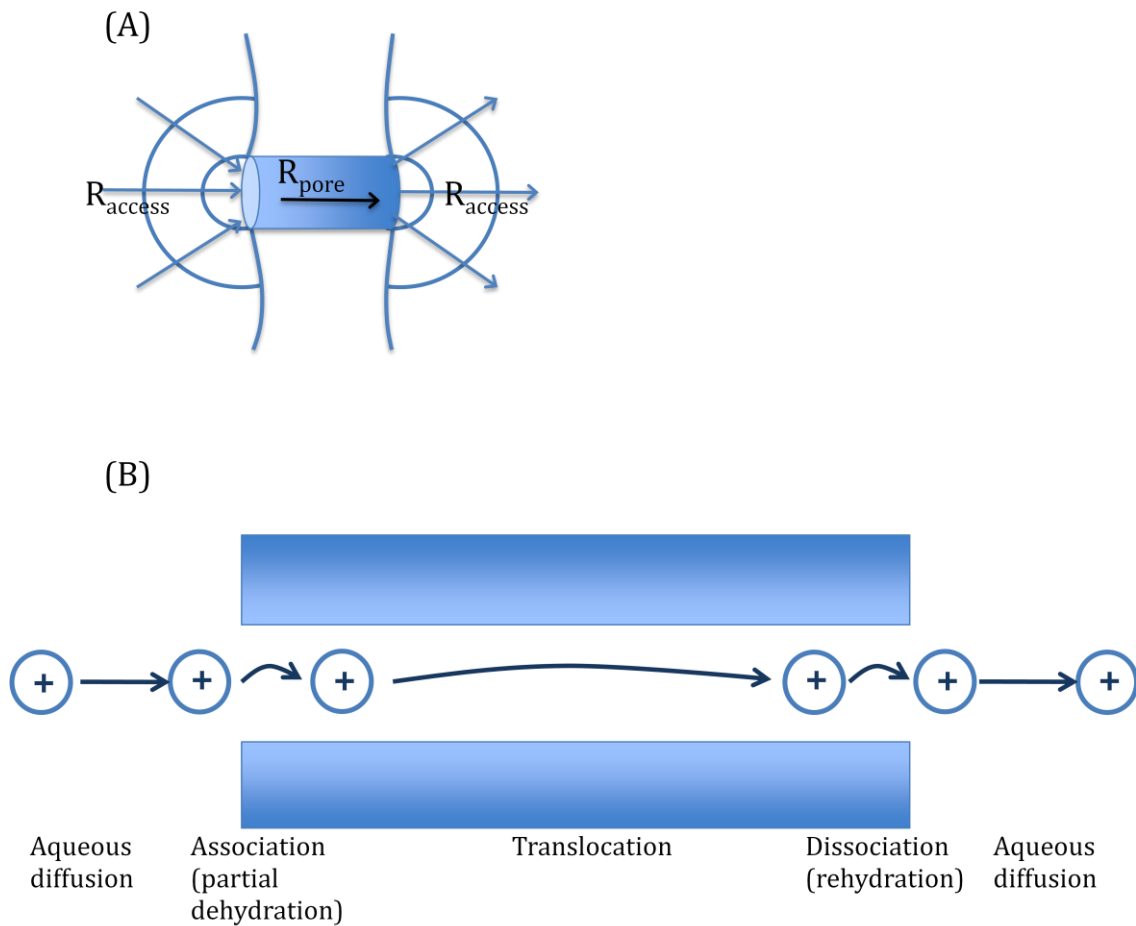


Figure 2.

A) Resistance across a membrane and through a protein pore. B) Steps of ion transport through a membrane protein pore. Redrawn from Hille, B. *Ion Channels Of Excitable Membranes*, p. 352 and 369.

Figure 2 illustrates the mechanics of proton movement through a membrane-inserted protein pore. Movement of ions (left to right) to the mouth of the pore constitutes the access

resistance, which corresponds to a “proton depletion zone” at the N-terminus of the M2 protein. Diffusion or translocation through the pore is the second step, the speed of which is used to distinguish between channel or transporter protein function. And at the far end—the right side of both figures, the C-terminus of M2 and interior of the proteoliposomes—the movement of ions away from the channel also contributes to the rate at which subsequent ions can move through the protein^{8,20}.

While proton channels such as gramicidin A or the artificially-synthesized “LS2” channel may not exhibit significantly higher proton conductance levels than transporters at low $[H^+]$ levels^{21,22}, they can be distinguished by “saturation” of proton flux at high $[H^+]$ ⁸. If inherent structural limitations of a protein prevent ion passage through the pore from increasing in direct relation to ion concentrations on either side of the pore, the flux through the protein will plateau, or “saturate” at the point where ion movement becomes protein-limited. This characteristic becomes a major distinguishing feature between proton/ion “channels” and “transporters.”

To investigate whether flux saturation was occurring with M2 in a liposome environment, this thesis project was designed to conclusively determine the basic characteristics of H^+ movement through the conductance domain of M2 (residues 22-62), elucidating:

1. H^+ flux into proteoliposomes at various pHs to distinguish between channel-type or transporter-type proton conductance;
2. Acid-activated conductance patterns, including determination of optimal pH;
3. Impact of concentration gradients, both of H^+ and other cations essential to the assay, on flux rate and liposome proton uptake capacity;
4. Amantadine efficacy in blocking H^+ flux at various pHs;
5. Functional integrity (determined via the above parameters) of the M2(22-62) truncate.

Using a novel M2 truncate of residues 22-62 (the transmembrane alpha-helix, plus a short, amphipathic “anchor” on the C-terminal end) developed by collaborators at Florida State University¹⁶, the research presented here validated the hypothesis that M2 functions as a proton transporter, rather than a traditional, proton-selective “channel”.

A portion of the results presented here have been reported previously^{20,23}.

EXPERIMENTAL DESIGN

Liposome Assay Introduction

The liposome assay, as mentioned above, allows experimentation at pHs outside of the range of physiological tolerance. Because M2 is a proton transporter, manipulation of extra- and intraliposomal pH is crucial to determining whether the protein is allowing H⁺ flux to occur in response to increased [H⁺], necessitating sometimes very acidic experimental pH. Another reason the liposome assay is so valuable is that, depending on liposome diameter, an artificial “cell” is created. The lipid bilayer surrounding this tiny sphere is composed of a natural cellular (*E. coli*) lipid extract, and when suspended in an aqueous solution, the lipids are associated with much the same tensile strength, bilayer thickness, and lipid fluidity that would be found in a natural cell. However, rather than having multiple other membrane proteins, cytosolic proteins, endo- and exocytotic activity, continual cell metabolism activity, etc. taking place constantly in order to maintain the membranous sphere, the lipids are thermodynamically stable all by themselves. The liposome can hold whatever buffer or salt solution the experimenter desires (as long as the osmolarity across the liposome membrane is balanced.)

Cell membranes act as capacitors *in vivo*, separating electrical charges associated with various ions and building up potential electrical energy across the membrane. Liposomal membranes are just as effective at this energy buildup, and in our proton flux assay we take advantage of that by building up a strong electrical gradient across the membrane. Once the liposomes are diluted into an osmotically balanced but K^+ and H^+ -asymmetrical solution, they contain a (relatively) high concentration of K^+ cations from KCl and potassium phosphate buffer. The overall charge inside the liposomes is balanced. But the K^+ -motive force is outwards, due to the very low (almost negligible) extraliposomal $[K^+]$.

Initially, without any means of transport across the membrane, K^+ is unable to follow its concentration gradient out of the liposomes. At this point in the experiment, M2 is present in the liposomal membrane (though only half of the M2 tetramers would be expected to be oriented correctly to pass protons into the spheres.) As soon as the liposomes are added to a solution of M2-active pH (<7) they're ready to begin allowing protons to follow *their* concentration gradient (from 75-fold to 10,000-fold, depending on extra-liposomal pH) and move into the liposomes. But as soon as one or two positively-charged protons pass that membrane barrier without bringing an anion with them, the charge inside the liposomes has built up to become so positive that the electrical repulsive force on H^+ equals the chemical gradient force, and Nernst equilibrium is reached. No protons can move until the potassium ionophore valinomycin is added to the experiment, which allows K^+ to leave the liposomes much more quickly than H^+ can enter them (meaning proton flux is not limited by any factor other than M2 structure). This actually produces a membrane potential, V_m that drives H^+ into the liposomes.

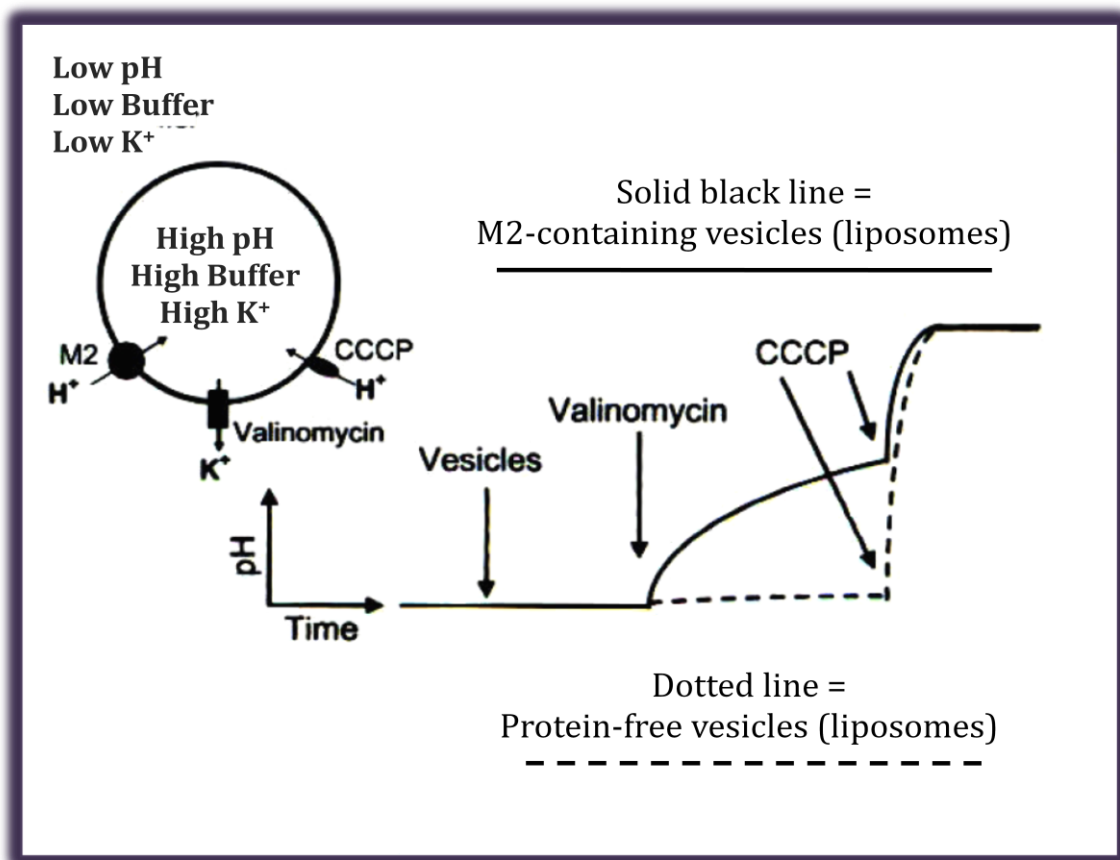


Figure 3.

Graphical representation of a typical proton-flux liposome assay. Large circle represents a single liposome, with internal solution elements listed. Proteins &/or ionophores (valinomycin, carbonyl cyanide 3-chlorophenylhydrazone) that can permeate the lipid membrane are shown, with the ions they transport and the direction of ion flux. The pH/time trace has arrows indicating addition of either liposome (“vesicle”) suspension or ionophore solution to the experiment.

The paradigm used consisted of two major elements: 1) composition/preparation of liposomes, and 2) the actual proton flux assay. Both the liposome preparation and liposome assay techniques were improved in small ways during the ~8 months between Set 1 (Oct. 2009, Jan-Feb. 2010) and Set 2 (July-Oct. 2010) of “activation-saturation” proton flux assays reported here. Changes were primarily in lipid/peptide drying and solubilization methods, and amantadine treatment, and are noted.

Proteoliposome composition/preparation

The M2(22-62) truncate used in these liposome assays included the transmembrane domain and post-transmembrane amphipathic helix²⁰. The construct, expressed in transfected *E. coli* BL21 (DE3), was comprised of an N-terminal 6-histidine tag followed by the large, soluble maltose binding protein, then a Tobacco Etch Virus-protease cleavage site, and finally the insoluble M2(22-62) peptide. The fusion protein was collected from the bacterial membrane fraction by solubilization with dodecylmaltoside, and purified via affinity chromatography with a nickel-nitriloacetic acid-treated agarose bead column. The peptide was cleaved from the fusion protein with TEV protease for 20 hours. The reaction mixture was precipitated with trichloroacetic acid and lyophilized. The cleaved M2(22-62) amino acid sequence was:

SNASSDPLVVAASIIGILHLILWILDRLFFKSIYRFFEHLKRG

The peptide was solubilized using methanol and the concentration determined by absorbance at 280 nm using a generic extinction coefficient ($1 \text{ ml mg}^{-1} \text{ cm}^{-1}$). It contained a fragment of the TEV cleavage site (Ser, Asn, Ala) at the N-terminus, such that the total length was 44 amino acids, with a calculated molecular weight of 5014.9 Da. Methanol-solubilized peptide was received in July 2009, aliquoted into ~1.5 mL portions, and stored long-term at -80°C or short-term at -20°C until use in October 2009, January-February 2010, and August-October 2010.

Desired size of a liposome “batch” was determined, and a corresponding amount of *E. coli* polar lipid extract (Avanti Polar Lipids) in chloroform was measured into an organic-solvent-washed and N₂-dried glass bulb or culture tube. Using the known protein concentrations of M2 protein truncate now suspended in a 50% methanol/50% chloroform solvent, protein was added to the still-suspended lipid (Set 1 of activation-saturation experiments, Figure 7), or, with

extra methanol, to a vacuum-dried thin lipid film (second set of activation-saturation experiments, Figure 8). If preparing “blank” (protein-free) control liposomes, only pure methanol was added. It was experimentally determined that the optimal protein-lipid ratio for these assays is 1:200 (Fig. 17, Appendix), which was adopted as the standard liposome composition ratio for these experiments. The still-suspended protein and lipid were then vortexed thoroughly, dried under N₂ to a thin film on the glass, then further dried under a vacuum for 1-2 hours (Set 1) or not (Set 2).

The extrusion filter apparatus was assembled and warmed in a 50-55°C incubator. Liposome internal buffer (description follows in “Proton flux assay design and execution” section) was also warmed to the same temperature. The mixture was heat-extruded: 1) to ensure that the sample was above the liquid-gel phase transition temperature of the lipid, allowing complete formation of lipid into properly sized liposomes, and 2) to facilitate ease of extrusion, as room-temperature extrusion frequently required enough force on the syringe plungers to rupture the thin polycarbonate filter membrane. The lipid-protein thin film was also warmed in the incubator to 50-55°C.

Warmed internal buffer was then added to the lipid/protein film, and the solution vortexed thoroughly (occasionally requiring up to 30 seconds of bath sonication to remove lipid from the glass walls), until visual confirmation established that all lipid and protein was suspended in the solution. The liposome suspension would appear quite milky at this point, due to the varied light diffraction by spontaneously-formed liposomes. This milky appearance was taken to indicate a predominance of liposomes of diameter larger than the wavelength of visible light, or >800 nm. The suspension was then passed 21 times (standard protocol for liposome extrusion) through an extrusion filter apparatus consisting of two glass gastight syringes affixed

to metal probes inserted into Teflon blocks, which are fitted into a metal housing that firmly sealed a porous polycarbonate filter membrane between the blocks. Either of two different units were used: Avestin LiposoFast Basic, Avestin, Inc., Ottawa, Canada and Avanti Mini-Extruder, Avanti Polar Lipids, Alabaster, AL, USA. Filter membranes of 100 nm diameter pore size were used, which yielded liposomes of uniform diameter from 120-150 nm, the majority being close to 130 nm, as determined by Dynamic Light Scattering (see below). Successful extrusion was also visually confirmed—as a qualitative, subjective determinant—by the observation that the extruded liposome suspension became much less opaque after extrusion.

Liposomes were used within 1-7 (Set 1) or 1-14 (Set 2) days of preparation, to avoid settling and aggregation of liposomes or possible protein deterioration. For amantadine sensitivity determination, a portion of the extruded liposome suspension was separated, and amantadine added to a concentration of 0.1 mM (Set 1) or 0.2 mM (Set 2). All samples were stored at 4°C.

All liposome batches were analyzed with Dynamic Light Scattering (“90Plus” instrument model, Brookhaven Instruments, Holtsville, NY, USA) for size uniformity. Test batches of liposomes were assayed for lipid & protein content after extrusion, to verify protein:lipid ratios and final concentrations in a typical batch. An assay for phosphate quantitation²⁴ indicated no significant difference in lipid present before extrusion or after extrusion with either brand of extruder (see Appendix). Protein assay efforts here were unsuccessful (see Appendix), but during my attempts a group of researchers shared results using a modified detergent-compatible commercial (BioRad DC Protein Assay) colorimetric protein assay to quantitate protein amounts in liposomes after extrusion, detergent-mediated lipid solubilization, and Bio-Bead treatment²⁵. Their data indicated that more than 95% of purified full-length M2 protein successfully

incorporated into mixed-phospholipid liposomes at pH 6.2 and above. Their method would have more avenues for protein loss than the method described here, and therefore this relatively simple extrusion method is assumed to be similarly protein-retentive.

Proton flux assay design and execution

The proton flux assay used here was based on the Franklin/Moffat/Woodbury proton uptake assay²⁶. As mentioned above, the assay utilized a high concentration of K^+ cations inside, relative to outside, the liposomes, which could efflux upon introduction of the K^+ ionophore valinomycin, carrying positive charge out to allow proton influx through M2. A second major characteristic of the intraliposomal solution was a relatively high buffer concentration, keeping the entrant protons bound and out of the way for new proton entry, essentially indefinitely, at the buffer concentrations used here. Flux measurements were taken from the initial 10 seconds of proton influx, when the intraliposomal buffer was far from Nernst equilibrium. Solution compositions were: internal liposome buffer: 50 mM KCl, 100 mM K^+ phosphate (half as K_2HPO_4 , half as KH_2PO_4), 320 mOsm, pH 8; external liposome buffer: 165 mM NaCl, 2 mM citrate (1.67 mM Na^+ citrate, 0.33 mM citric acid), 330-340 mOsm. The external buffer solution was titrated appropriately (with HCl or NaOH) to bring experimental pH to 6.5, 6.25, 6.0, 5.75, 5.5, 5.25, 5.0, 4.75, 4.5, or 4.0 after addition of 1% volume of liposomes in internal buffer. For example, for experimental conditions of pH 6.5, the external buffer pH alone had been titrated beforehand to 6.0, and addition of liposomes at pH 8 brought the experimental pH up to 6.5. For a pH 4.0 experiment, external buffer of 3.5 initial pH was used; and so forth for all other pH values. Osmolarity of external buffer, even after re-titration to a few different pH values, did not exceed 340 mOsm.

The external liposome buffer was osmotically balanced with the internal by using NaCl, which supplied anions impermeant to the liposomes. Protein-free, “blank” liposome control preparations were also tested, showing less permeability to K^+ and greater resistance to depolarization. When testing liposomes incubated in 0.1-0.2 mM amantadine, amantadine solution (30 μ L of 10 mM) was added to the 3 mL external buffer “bath” to maintain amantadine concentration at 0.1 mM once the liposome aliquot was diluted into that buffer.

At initiation of the assay, the pH microelectrode was placed in the 3 (or 3.03, if amantadine was added) mL bath of external buffer. pH changes were recorded as voltage changes, measured with a pH meter having its output connected to a -100-gain amplifier with variable offset such that voltage equaled offset plus 5.7 volts per pH unit. The voltage changes were tracked with an analog-to-digital converter installed in a computer using the LabView data acquisition program, and the experimenter also noted the reading from the pH meter at crucial points during the experiment (for comparison and to register the DC offset employed). After tracking any slight pH changes or equipment-induced voltage change (“drift”) for 1-2 minutes, an aliquot of 30 μ L of liposomes was injected into the rapidly stirring solution. Since the liposomes were suspended in internal buffer and only trapped ~5% of the volume, they added a nearly 100-fold dilution of internal buffer to the composition of the now-3.03 (or 3.06) mL external buffer volume. (The resulting pH change was accounted for in the composition of the external buffer, as noted above.) Amantadine was measured to have a negligible effect on pH when added to the bath.

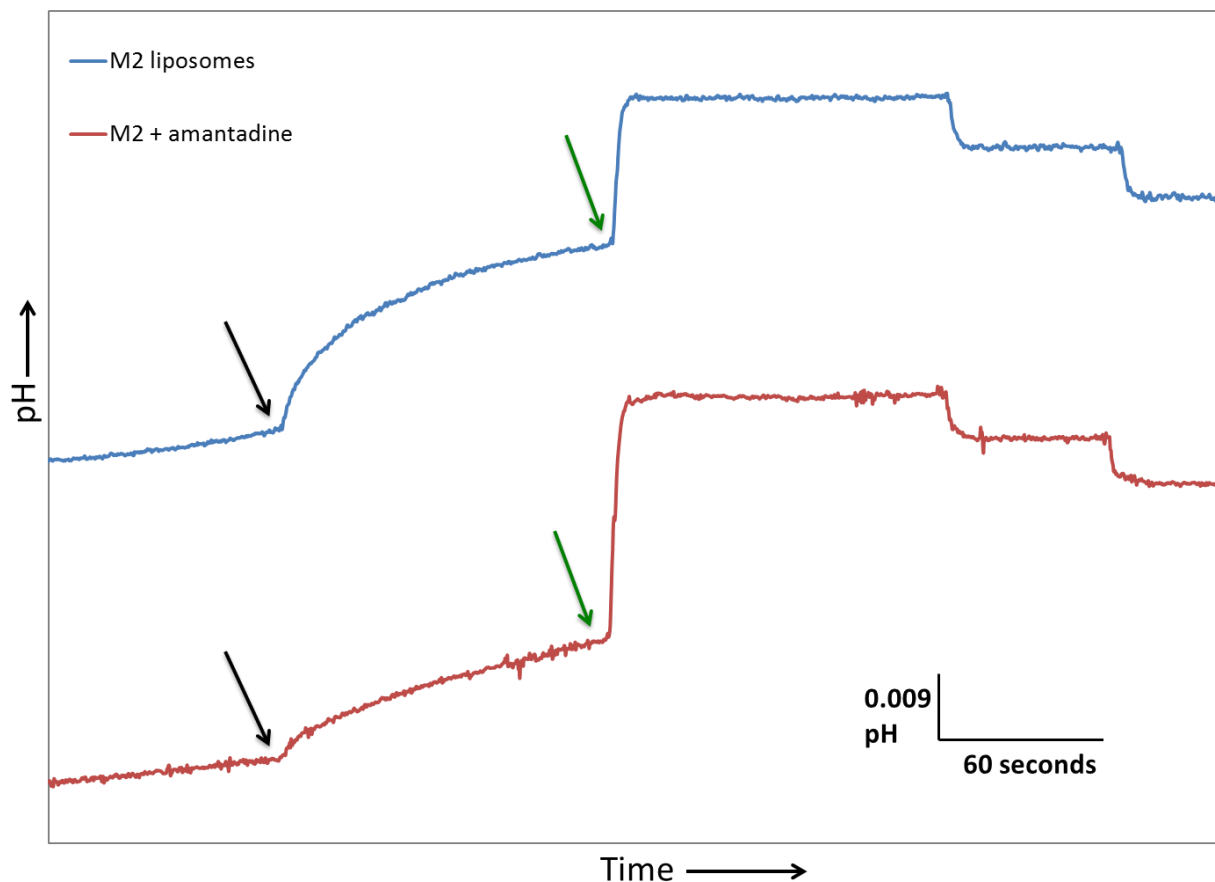


Figure 4.

Raw pH/voltage change data plotted over time for two proteoliposome proton flux assays at pH 6.5 (from experiment Set 1). Liposomes were comprised of 0.1 mg M2(22-62): 20 mg E.coli lipid extract: 1 mL internal buffer. Upper left corner legend identifies proteoliposomes only (blue trace) and proteoliposomes incubated and assayed in 0.1 mM amantadine (red trace). Key time points in the experiment are indicated with arrows: valinomycin injection (black), CCCP injection (green), two back-titrations of 30 nEq each of HCl (purple). Traces were vertically offset for comparison purposes.

After allowing 1-2 minutes for full equilibration of the bath and to track any drift seen in the presence of the liposomes, 4 μ L valinomycin (in ethanol) was injected into the bath. This amount was calculated based on the lipid amount used and size of the liposomes. With 10 mg of lipid at about 750 g/Mol, factoring in that each molecule had an average headgroup size of 0.64 nm^2 , the total lipid surface area would be $6.4 \times 10^{17} \text{ nm}^2$. With 100 nm-diameter liposomes, that translated to 2×10^{13} liposomes in a 0.5 mL liposome preparation. In 30 μ L (one experiment),

then, there would be 1.22×10^{12} liposomes. These experiments employed 4 μL of 25 $\mu\text{g/mL}$ valinomycin (in ethanol), with a formula weight of 1111.36 g/Mol. That amount would yield 5.3×10^{13} molecules of valinomycin per experiment, meaning that there were about 43 valinomycin molecules per liposome, more than enough to keep K^+ transport from being rate-limiting.

Depending on which liposomes were being tested, the pH (and hence, voltage recorded by the amplifier) would rise precipitously or only slightly, but always “leveled off” within about one minute of valinomycin addition. An additional minute was allowed to pass, then 25 μL of 200 mM CCCP (also in ethanol), a protonophore, was injected into the bath. This proton transporter maximized the proton influx capability of the liposomes, giving a measurement that reflected the total proton-uptake capacity of all liposomes in the experiment. The CCCP volume used was, as with valinomycin, based on the calculated number of liposomes in the experiment. 25 μL of 200 μM CCCP, added to the 1.22×10^{12} liposomes in the experiment, provided 3×10^{15} CCCP molecules per experiment, or 3000 CCCP molecules for every liposome.

A pH/voltage maximum was reached very quickly (within 10 seconds) after CCCP addition. After a two-minute recording of this *very* stable pH plateau, 30 nanoMoles of H^+ (as HCl) were injected into the vial (30 μL of 1 mM HCl), referred to as a “back-titration.” As the liposomes were then fully permeable to protons, the buffer inside them had effectively become part of the overall bath. When a measured number of protons in the form of HCl were then added, then ensuing pH/voltage change could be used as a gauge to calibrate proton influx into the liposomes. The addition of 30 nanoMoles of HCl was repeated a second time, post-hoc additions of valinomycin and CCCP were made to test their direct effects on pH, and the experiment was concluded.

Data extraction

Using Microsoft Excel, data points were hand-selected (see Fig. 5) from the data trace to calculate proton flux at various key time points during an experiment. First, the two back-titration voltage differences were calculated and averaged to give the pH electrode voltage (in mV) for exactly 30 nanoMoles of H⁺ flux. This could vary with buffer titration, so it was important that pH change be restricted to a narrow range, within a few hundredths of a pH unit from the other measurements in the experiment.

Next, a 10-second set of data points was taken, beginning just after the valinomycin peak and ending 10s into the peak, to calculate the initial slope of voltage change upon addition of the potassium ionophore. The following formula was used to fit the data progression from steep curve to gentler rise during these 10 seconds:

$$m = \frac{N \sum x_i y_i - \sum x_i y_i}{N \sum x_i^2 - (\sum x_i)^2} \quad (1)$$

This enabled calculation of the initial proton-influx slope, or “initial slope,” which was decided upon as being the most important quantitative measurement of M2 H⁺ conductance.

The slope of the trace immediately *before* valinomycin addition was also calculated, to provide a measurement of the small, usually upward/basic pH drift from slow depolarization of the liposomes due to leak conductance of K⁺. This pre-valinomycin drift was subtracted to correct the raw valinomycin initial slope. To correct for artifactual voltage changes induced by injection of the ethanol-suspended ionophores, post-hoc valinomycin and CCCP injections were also carried out for the experiments in Set 2.

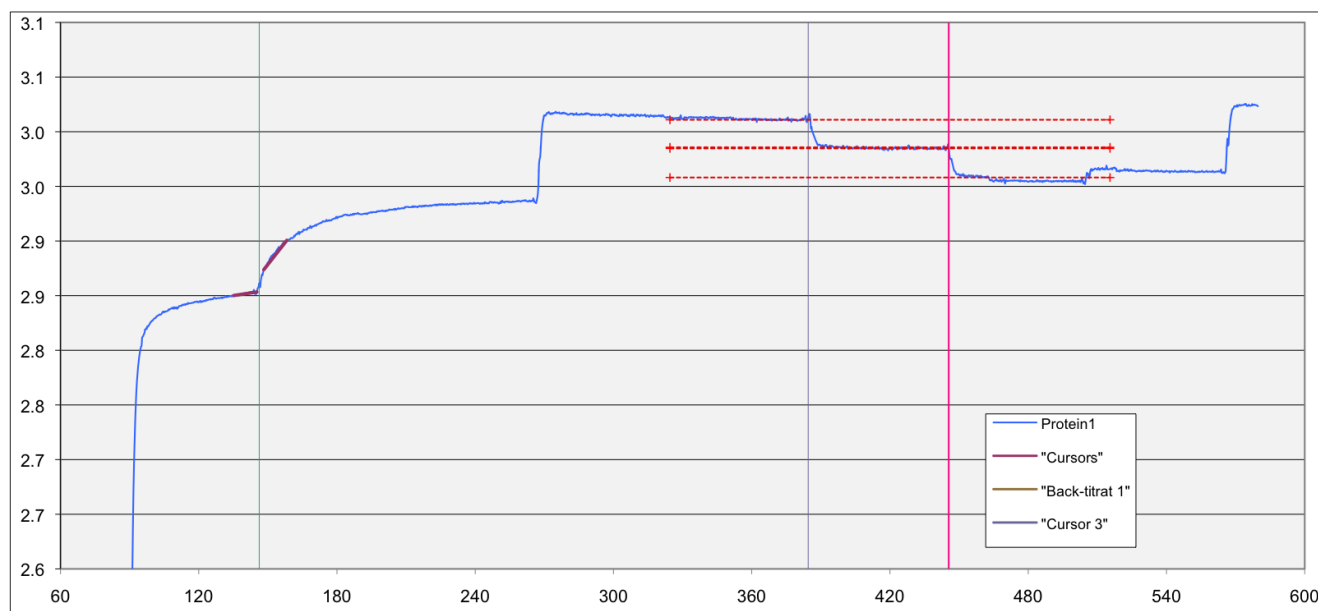


Figure 5.

Liposome assay from Set 2 showing typical analysis protocol. Experimental pH_o 6.0, liposome suspension of 0.1 mg M2(22-62): 20 mg E.coli lipid extract: 1 mL internal buffer, pH_i 8.0. Voltage change (y axis) plotted against time in seconds (x axis) in Microsoft Excel for analysis. Green cursor (~145s) was placed at valinomycin peak, with red bar to the left showing data points being averaged to obtain pre-valinomycin “drift” slope, and red bar to the right showing data points averaged (via Equation 1) from 2s post-valinomycin to obtain initial slope. The faint purple and bright pink cursors were placed at the beginning of both HCl back-titrations to calculate the voltage change from pre-cursor to post-cursor, yielding two values for the voltage change induced by 30 nEq of H^+ . Dotted red lines aided in accurate placement of back-titration cursors.

The calculated valinomycin-induced voltage change was then related to H^+ flux, or pH. Dividing the valinomycin slope by the average ΔV for 2 back-titrations of 30 nmoles HCl each yielded a H^+ flux value in units of 30 nM H^+ /sec, which was converted to units of H^+ /second. However, this value was comprehensive for the proton flux from all M2 tetramers in all liposomes in the experiment. Dividing by the number of nanoMoles of tetramers of M2 in that sample gave a per-tetramer value for M2 conductance.

One final correction was necessary: because the liposomes were artificially mixed and assembled, we followed the example of previous liposome investigations and assumed that half

of the tetramers present were oriented C-terminus-out²⁷, which is a primarily non-conducting state (though voltage clamping of MEL cells did indicate some C-to-N proton backflux when concentration and electrical gradients were oriented favorably¹⁴). The newly-described detergent-to-lipid BioBead-mediated solubilization of extruded liposomes was shown via mass spectrometry in a recent study to produce liposomes with *all* M2 protein oriented N-terminus-out²⁵, but our methods were different enough to render an assumption of similar orientation inapplicable to the data presented here. It was assumed that the basic pH inside the vesicles would block proton uptake by the 50% of tetramers whose N-termini were inside the liposomes, so that H⁺ conductance was carried out only by the remaining 50%. The calculated per-tetramer conductance was therefore multiplied by 2, to account for the presumed half (by quantity) activity of the protein. This final step yielded the proton flux per active tetramer, as reported here.

Analysis

An equation describing electrodiffusive behavior in a channel at a fixed membrane potential is:

$$J_{H^+ in} = P[H^+]_{out} \quad (2)$$

where P is permeability of the channel for the “fixed conditions.” An equation describing saturating transporter activity is:

$$J_{H^+ in} = \frac{J_{max}}{1 + \frac{k_d}{[H^+]_{out}}} \quad (3)$$

$J_{H^+ in}$ is the influx (net of “fixed” efflux). The denominator in equation 3 represents the probability of a multiply protonated histidine residue within the protein prepared to release a

proton to the interior. The data, measured at various values of $[H^+]_{out}$, will be compared to these two predictive functions. The null hypothesis, “no saturation of transport rate,” will be rejected if the χ^2 value for the best fit of equation 3 statistically excels compared to that for the best fit of equation 2.

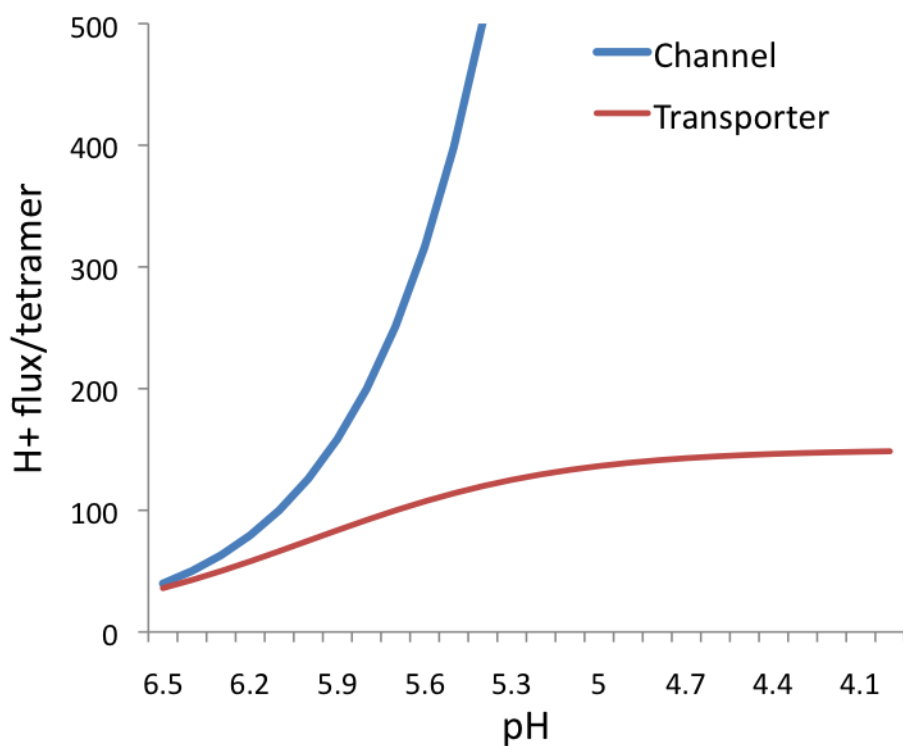


Figure 6.
Proton flux vs. pH.

Figure 6 shows the distinctive curves yielded when plotting H^+ flux per M2 tetramer against pH for either a proton channel (equation 2) or a transporter (equation 3).

RESULTS

Proton Flux, Acid-Activation, and Amantadine Block Quantitation

Results of a range of liposome proton flux experiments performed October 2009 and January-February 2010 at pHs ranging from 6.5 to 4.0 are plotted in Figure 7. Upon comparison to Figure 6, the data more closely approximate a transport-characteristic, rather than channel-characteristic, binding curve.

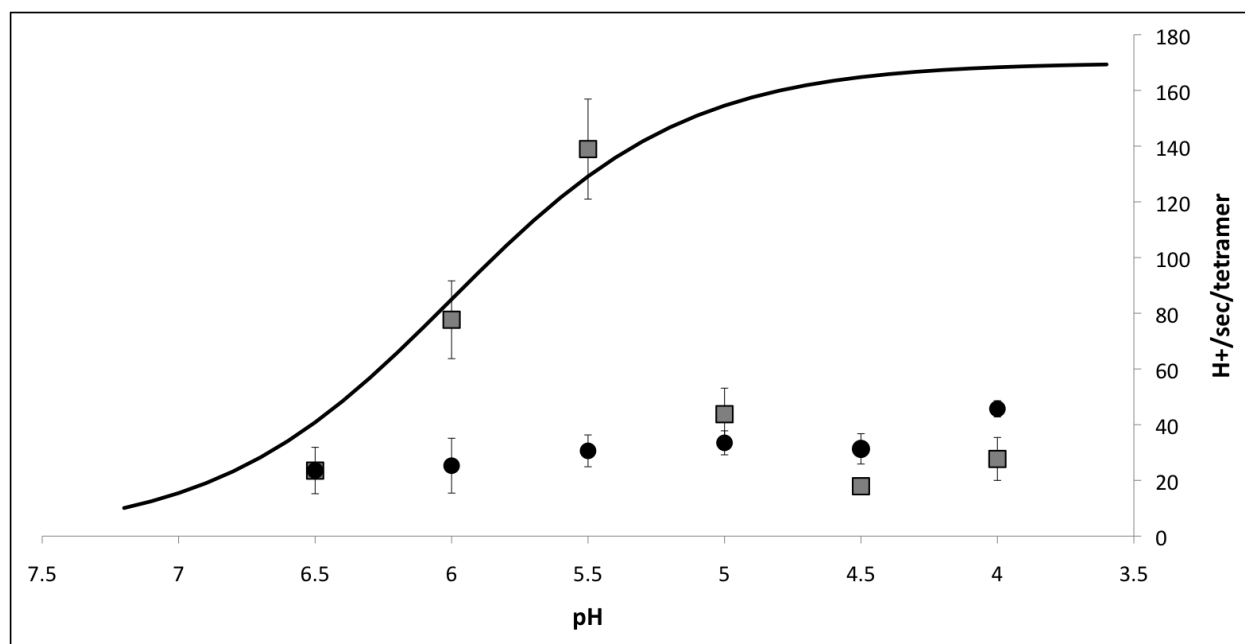


Figure 7.

Set 1 of activation-saturation experiments with M2(22-62) proteoliposomes (squares). Proton flux measurements were done with pH_o of 6.5 to 4.0, $\text{pH}_i = 8.0$. 0.1 mg M2(22-62):20 mg lipid:1 ml internal buffer liposome suspension was diluted 100-fold into pre-pHed, isoosmotic external buffer containing citrate. For experiments with amantadine (circles), liposomes were incubated in 0.1 mM amantadine overnight, and external buffer contained 0.1 mM amantadine as well. Proton flux measurements were corrected for baseline H^+ leakage into the liposomes prior to valinomycin addition, and for valinomycin-induced H^+ leak observed in protein-free liposomes. Fluxes are doubled as a correction for protein orientation and gating. The saturation curve was fitted with a pK_a of 6.0, a maximum flux of 170 H^+ /second/tetramer from eq.3. The error bar for each point represents ± 1 S.E., calculated as the square root of the sum of the standard errors of the means for the test group and the control (protein-free liposomes) group. From left to right, $N=6, 5, 6, 9, 8,$ and 4 for the protein; $N=3, 3, 2, 3, 3,$ and 3 for the amantadine experiments. Nominal membrane potential: -114 mV.

Proton flux increased with decreasing pH_o down to pH 5.5, but then dropped abruptly at lower pHs. Amantadine blocked ~80% of proton flux at pH 5.5. At pH 6.5, the interexperimental errors were too large to detect block in this set of experiments. Protein desensitization below pH 5.5 rendered detection of amantadine block difficult. Protein-free liposome fluxes were small (~1 H^+ /tetramer-s, calculated as if protein were present, data not shown) and were subtracted. Transport rose following a theoretical binding curve having a pK of 6.0, and a maximum flux of 170 H^+ /tetramer-s.

A second set of experiments to validate the findings in Figure 7 was executed in July-October, 2010, at some of the same pH points but also including data at intermediate pHs for refinement of the acid activation and flux saturation patterns previously observed (Figure 8).

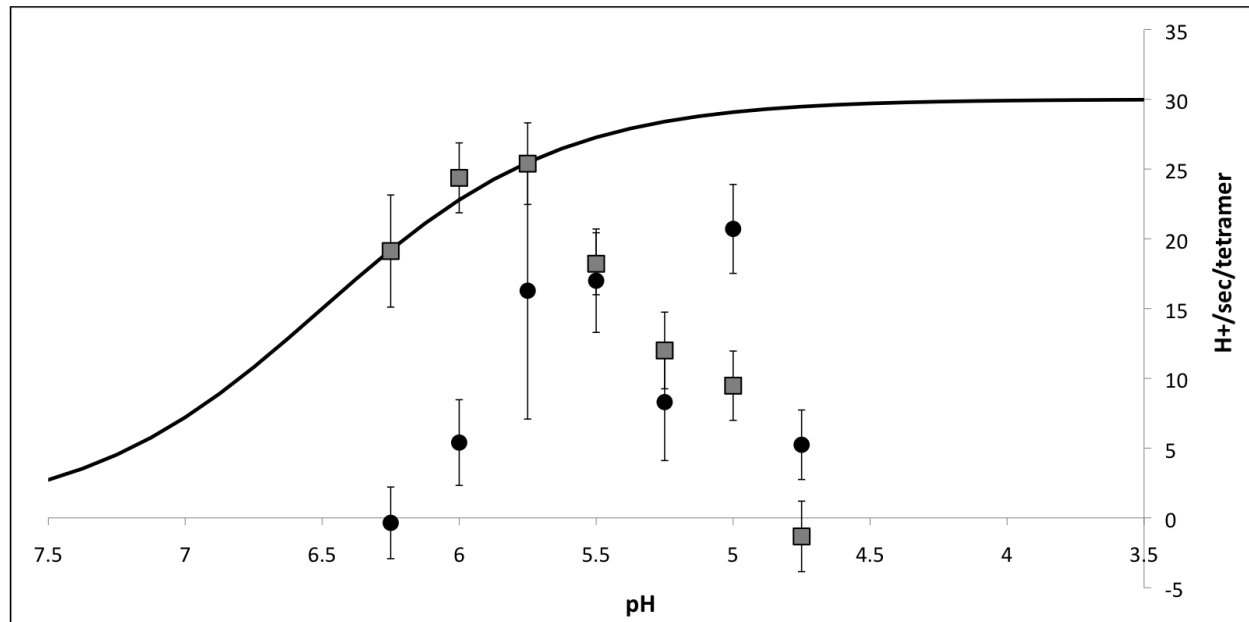


Figure 8.

Second set of activation-saturation experiments with M2(22-62) proteoliposomes (squares). Proton flux measurements were done with pH_o of 6.25 to 4.75, $\text{pH}_i = 8.0$. 0.1 mg M2(22-62):20 mg lipid:1 ml internal buffer liposome suspension was diluted 100-fold into pre-pHed, isoosmotic external buffer containing citrate. For experiments with amantadine (circles), liposomes were incubated in 0.2 mM amantadine overnight, and external buffer contained 0.1 mM amantadine. Proton flux measurements were corrected for baseline H^+ leakage into the liposomes prior to valinomycin addition, and for valinomycin-induced H^+ leak observed in

protein-free liposomes. Fluxes are doubled as a correction for protein orientation and gating. The saturation curve was fitted with a pK_a of 6.5, a maximum flux of 30 H^+ /second/tetramer. The error bar for each point represents ± 1 S.E., calculated as the square root of the sum of the standard errors of the means for the test group and the control (protein-free liposomes) group. From left to right, $N=9, 8, 8, 11, 8, 7, 8$ for the protein; $N=6, 5, 5, 5, 4, 5, 6$ for the amantadine experiments. Nominal membrane potential: -114 mV.

Results of the second set were similar to those in Figure 7. Proton flux increased with decreasing pH_o to 5.75, but then began to drop between pH 5.75 and 5.5. With amantadine present, the flux was 100% blocked at pH 6.25. Amantadine block was reduced to near 0% at pH 5.5. Protein-free liposome fluxes ranged from 4 H^+ /tetramer-s at pH 5.75 to 17 at pH 4.75 and were pre-subtracted from protein flux raw data. Transport rose following a theoretical binding curve having a pK of 6.5, and a maximum flux of 30 H^+ /second/tetramer.

Measured peak proton flux rates through M2(22-62) in these liposome assays were 139 (Set 1) or 25 (Set 2) to protons per second per tetramer. The upper value exceeds any previously published^{5,26,27}, although a recent study using the full-length M2 protein and quantifying flux via intravesicular Glu³ fluorescence reported rates of 45 protons/second/tetramer²⁵.

A somewhat unexpected finding was the observation that the M2(22-62) truncate seemed to lose function below pH 5.5-5.75, as evidenced by an abrupt drop in proton flux at low pHs and reduction (or elimination) of amantadine block, often with higher flux into amantadine-bound proteoliposomes than untreated ones. Figures 10 and 11 below show raw data following the pH change through the time-course of a proton flux assay, first with robust proton uptake and amantadine block at pH 6.5, then severely reduced uptake and block at pH 4.5. These traces, though individual, were typical of experiments at those pHs.

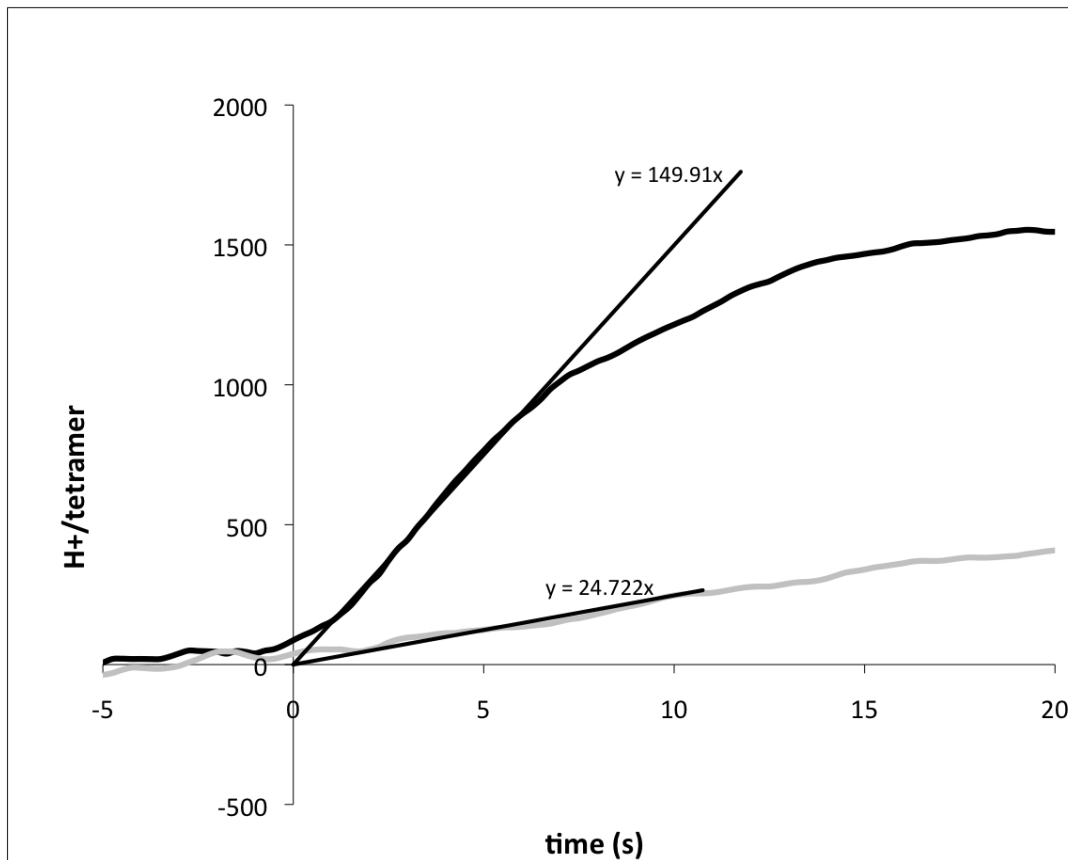


Figure 9.

Proton uptake per tetramer as a function of time, in the absence (black) and presence (gray) of 100 μM amantadine. $\text{pH}_{\text{ex}} = 5.5$, from experiment Set 1. The initial slopes (lines), after protein-free liposome proton flux subtraction and pre-valinomycin drift subtraction, were 140 protons per tetramer per second and 30 protons per tetramer per second, respectively, corresponding to $\sim 80\%$ blockage by amantadine²³.

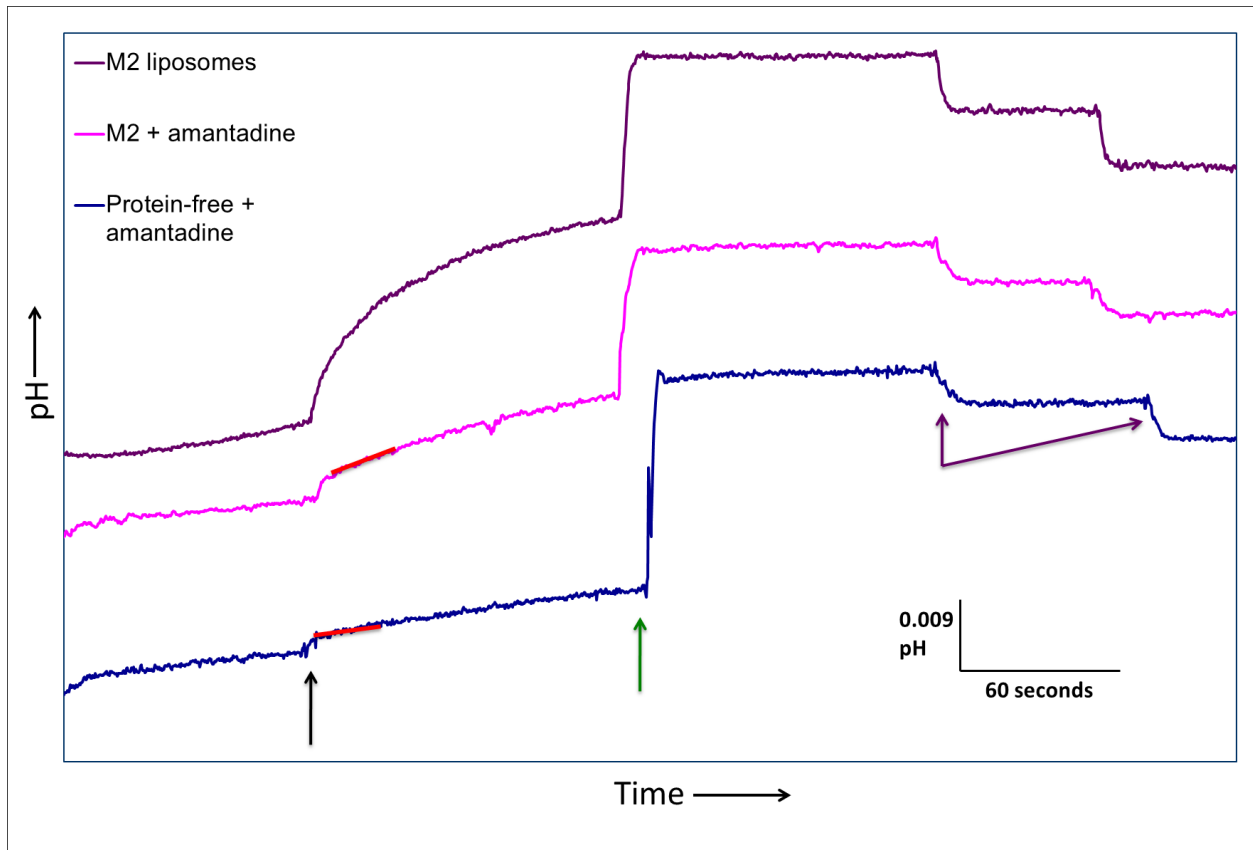


Figure 10.

Raw data traces from the first set of activation-saturation liposome assays. Experiments were at pH 6.5. Upper left corner legend identifies proteoliposomes only (maroon trace), proteoliposomes incubated and assayed in 0.1 mM amantadine (pink trace), and protein-free liposomes incubated and assayed in 0.1 mM amantadine (blue trace). Arrows indicate: valinomycin injection (black), CCCP injection (green), two back-titrations of 30 nEq each of HCl (purple). Red bars follow the approximate initial slope after valinomycin addition, highlighting proton flux differences between amantadine-blocked and amantadine-free M2(22-62), with all three cases showing baseline slow depolarization. Traces were vertically offset for comparison purposes.

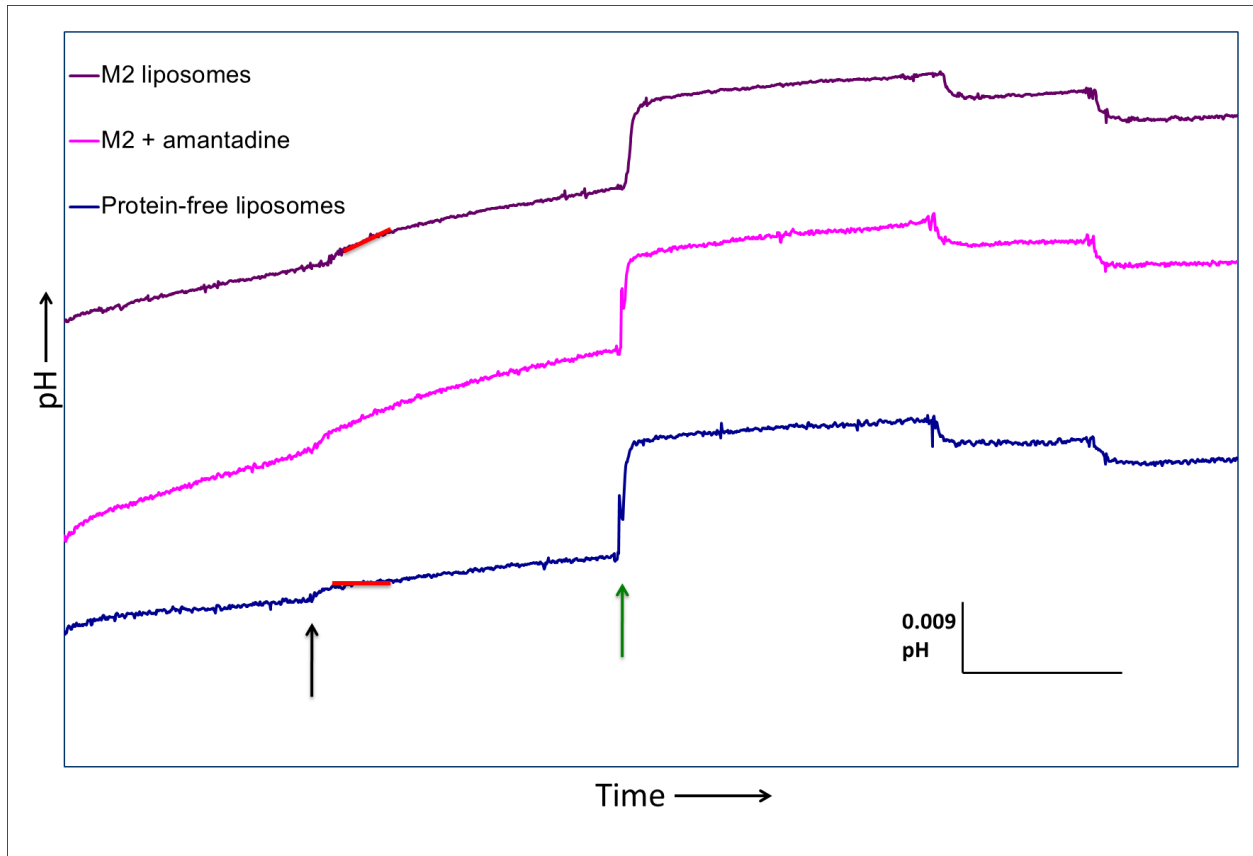


Figure 11.

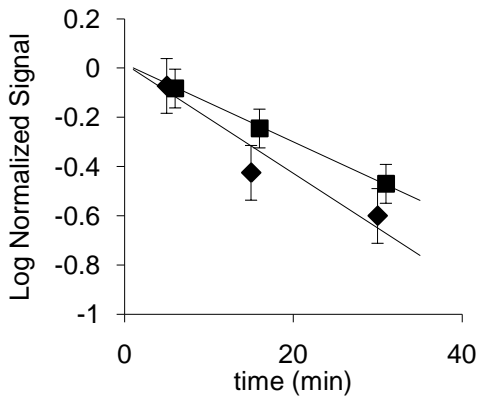
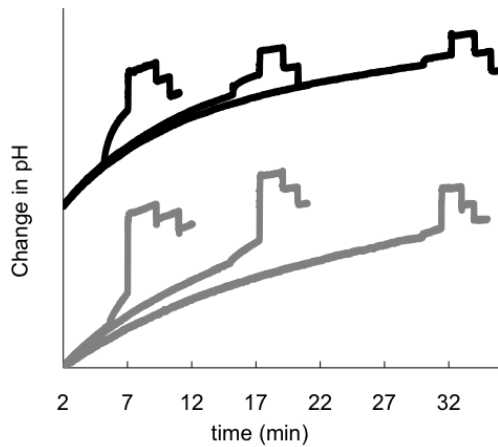
Raw data traces from the first set of activation-saturation liposome assays. Experiments were at pH 4.5. Upper left corner legend identifies proteoliposomes only (maroon trace), proteoliposomes incubated and assayed in 0.1 mM amantadine (pink trace), and protein-free liposomes (blue trace). Arrows indicate: valinomycin injection (black), CCCP injection (green), two back-titrations of 30 nEq each of HCl (purple). Red bars follow the approximate initial slope after valinomycin addition, highlighting proton flux differences between amantadine-blocked and amantadine-free M2(22-62), with all three cases showing baseline slow depolarization. Traces were vertically offset for comparison purposes.

Factors to consider when interpreting Results

Limited, low-level alkali metal transport by M2 was suggested to be physiologically valuable for virus acidification in the recent Leiding/Årsköld study²⁵. Here, quantification of slight K⁺ “leak” through M2(22-62) was fully implemented, giving an improved estimate of M2(22-62) selectivity and exploring the time course of vesicle depolarization by M2 transport of K⁺. The small amount of citrate buffer (citric acid and sodium citrate) present in the external

buffer solution was intended, initially, to reduce a steady upward pH drift observed in the first experiments and believed to be due to CO₂ diffusion into the rapidly stirring, originally-unbuffered solution. However, liposome depolarization time course experiments (Figure 12) and

A



B

Figure 12.

A) pH traces with varying delays after acidification to evaluate total liposome proton-uptake signal rundown, (the sum of the valinomycin and the CCCP uptake signals). Each trace is representative of a set of three equivalent experiments. pH traces for protein-containing (black) and protein-free (gray) liposomes were aligned vertically to start at different levels (at the arbitrary reference time of t=2 min) for ease of comparison. The exact pHs at the time of valinomycin addition were, from left to right: 6.147, 6.185, 6.173 (protein traces) and 6.160, 6.153, and 6.194 (protein-free traces). The start time is designated as the time of bath acidification, which establishes a pH gradient but should only cause minimal H⁺ flux in the absence of K⁺ transport. 0.1 mg M2(22-62):20 mg lipid:1 ml internal buffer diluted 100-fold into citrate-free external buffer. Protein-free-liposome-subtracted specific activity at t=5 minutes:

19±4 H⁺/tetramer-s (N=2; pH_o 6.2). B) Logarithmic representation of total liposomal proton uptake (representing total trapped volume). Diamonds (laterally offset for clarity) represent proteoliposomes and squares represent protein-free liposomes. Total signal, corrected for artifacts (measured separately) due to addition of ethanolic valinomycin and CCCP, was normalized by extrapolation of the assumed exponential decay to 0-time total uptakes of 143±4 nEq H⁺ (proteoliposomes) and 200±40 nEq H⁺ (protein-free liposomes). Total heights were corrected by subtraction of a small proportion, 15 nEq H⁺ (one half the back titration pH change) in each case, to compensate for pH changes observed upon addition of the effectively alkaline ethanolic reagents (valinomycin and CCCP), to liposome-free buffer. Error bars for each point represent ±1 SD, N=3²⁰.¹

liposome-free pH-change tests (data not shown) indicated that the initial pH drift could only be due to slight M2-induced K⁺ permeability of the liposomes. The rate of total signal decay was used to indicate the rate of depolarization of liposomes deriving from K⁺ permeability. Because trapped volume varied between liposome preparations, this required normalization of the total signal heights extrapolated back to the time when the liposomes were first exposed to a pH gradient (unlike the activation-saturation experiments, these assays' higher-pH, citrate-free external buffer required activating M2 by addition of HCl to bring pH down to a more-conductive level.) The total pH change/voltage signals from each experiment, corrected for ethanolic ionophore injection artifacts, were first fitted with an exponential decay function and then divided by the respective zero time (time of external buffer acidification) intercept for trapped volume normalization before averaging with the other two experiments in its group. The normalized averages were then fit with a unity-amplitude exponential decay function (solid lines on the semi-log plot), the characteristic time of the protein-free liposome curve was subtracted from the proteoliposome curve, and the result was multiplied by the zero-time intercept for the protein-containing liposomes to obtain the denormalized decay due to K⁺ flux (nmol K⁺/minute) through M2(22-62). This was then divided by the total protein content in the sample (0.15 nmol

¹ Results obtained by colleagues under my supervision. See acknowledgements.

tetramers) and converted to units of seconds. The difference between the protein-containing and protein-free liposomes' K^+ leak/ H^+ uptake slopes was presumed to be due to different decays during the 3 minute period between dilution and acidification, which apparently was greater for the M2(22-62) liposomes than the protein-free liposomes, (also self-consistent with the steeper slope for M2(22-62) liposomes). The normalization thus corrected for unequal initial effective total trapped volumes at the time of acidification.

Inter-experimental variation in the shape of the valinomycin and CCCP peaks, the baseline drift, and to a lesser extent in the shape of the back-titration pH drop were observed during all liposome assays, both the activation-saturation type and the K^+ depolarization assays described above. The shape of the back-titration was used to identify variations in stirring. Typically, the back-titration-induced pH/voltage change settled in about 2 seconds.

Initial flux was calculated from the linear portion of the valinomycin peak, within 2-7 seconds post-valinomycin injection. This approach was based on the assumption that the valinomycin peak shape was a single exponential, but in some experiments there appeared to be multiple exponentials, perhaps representing embedded compartments. Substantial baseline drift before addition of valinomycin was also common, likely due to the inherent lipid permeability to both protons and potassium ions.

In addition to variations in pH/voltage signal shapes, two major sources of uncertainty might have affected specific proton (or even K^+) flux estimates: liposome integrity and protein functionality. Liposomes were assumed to have been largely impermeable to protons/ions, enabling them to maintain a membrane potential. In protein quantification, any M2(22-62) not forming parallel tetramers (monomers, dimers, surface-associated protein, protein dissolved in water or lost in extrusion) would not have contributed to overall H^+ flux, though calculations

would have included it as being functional. There was also some decay in the polarization of the vesicles after dilution and/or acidification and decay in the apparent initial flux during the dead time. These uncertainties would all have led to underestimation of the specific H⁺ flux through M2(22-62), so the values presented here represent lower bounds.

Finally, amantadine binding to lipid was considered only after activation-saturation experiment Set 1 was completed. In those experiments, reported aqueous amantadine concentrations may have been reduced by ~1.7%, after calculations based on the partition constant of amantadine in charged phosphocholine bilayers being 84²⁸, and E. coli lipid possessing a similar amount of charge. For activation-saturation experiment Set 2, liposomes were incubated in 0.2 mM amantadine and the external buffer bath was brought to 0.1 mM amantadine before liposome addition.

DISCUSSION

Functional Characteristics of M2(22-62)

This research was designed to help resolve the question of whether M2 functions more as a traditional proton channel, or instead conducts protons in an ion “transporter” fashion. If the protein were to act as a channel by opening in response to acidic pH and remaining open (continuously or intermittently) as a proton floodgate, expected results would include:

- 1) No saturation of proton flux rate observed. Although channels with obligatory ion binding sites can saturate, protons shuttled by Grotthus conductance via a water wire would not.
- 2) Flux rate would increase as predicted by protein pore diameter and concentration/electrical gradient alone.

3) Little or no H⁺-selectivity.

If M2 behaved in the liposomes as a transporter, observations would yield:

- 1) Proton flux increasing as acid-activation point or p_k (about pH 5.8) was reached.
- 2) Flux would keep increasing to a point, likely somewhere between pH 5.8 and 5.0, then plateau to a level rather than continue to rise with [H⁺]. This would be the key “saturation” point or maximum rate at which a transporter could move ions, regardless of concentration/electrical driving forces. Proton conductance that was H⁺ selective.

This transporter-characteristic behavior was experimentally investigated and indicated by data from the proteoliposome proton flux assays reported here. Measured proton flux rates through M2 increased to pH values between 6.5 and 5.5, where the flux then ceased increasing. The pK of transport, or the point at which proton flux is no longer access-limited but rather translocation-limited, was determined with the saturation curves in Figures 7 & 8 to be 6.5-6.0. One limitation of the results presented here, however, was the loss of most or all proton transport function below pH 5.5. While full-length M2 in mouse erythroleukemia cells yielded proton conductance data down to pH 4¹, this truncated version lost H⁺ transport capacity at low pH.

This fall of activity below pH 5.0-5.5 is consistent with the pH dependence of tetramerization observed by Salom, et al, whose analytical ultracentrifugation studies using an M2 transmembrane domain peptide (“M2 TMD,” residues 22-46) reported an increasing prevalence of disassociated M2 TMD monomers relative to tri- or tetramers as pH decreased²⁹.

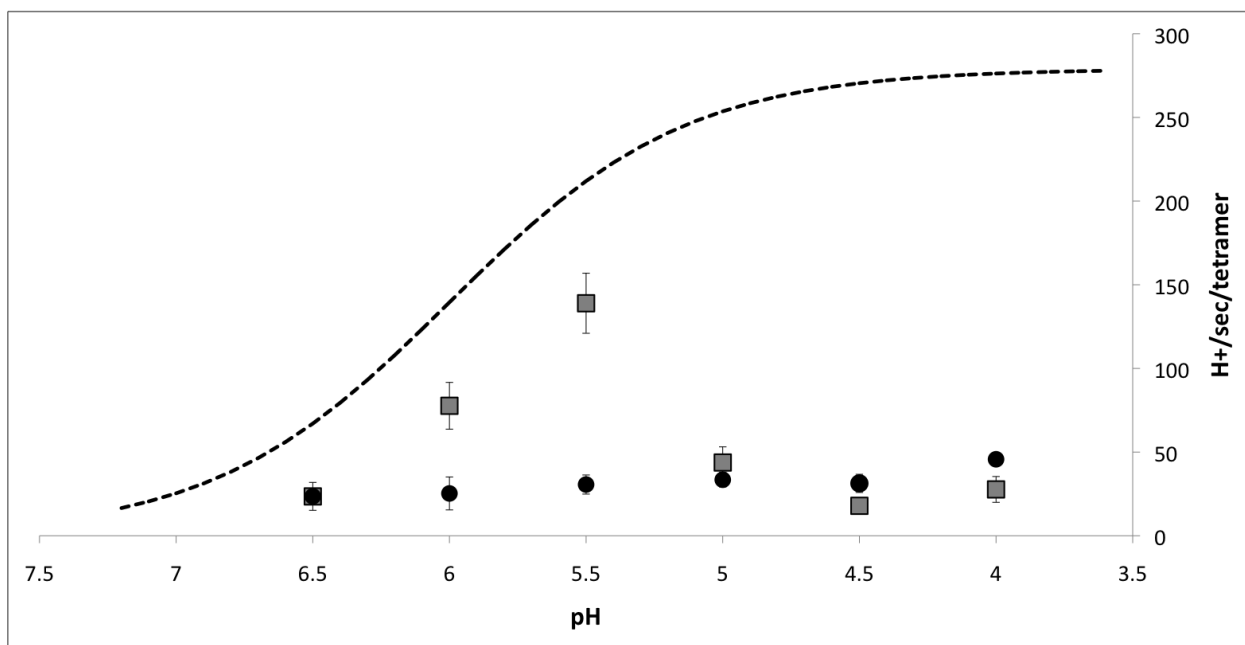


Figure 13.

Relation of Set 1 activation-saturation data to per-channel flux rates observed in *Xenopus* oocyte whole-cell voltage clamp assays. Dotted line represents a saturation curve with per-tetramer J_{\max} of 279 protons, and a pK of activation of 6.0. As in Fig. 7, gray squares indicate proteoliposome proton flux averages, and black circles indicate amantadine-incubated proteoliposome proton flux averages. Measurements were corrected for baseline H^+ leakage into the liposomes prior to valinomycin addition, and for valinomycin-induced H^+ leak observed in protein-free liposomes.

The Salom study also showed enhanced tetramerization of M2 monomeric subunits in the presence of amantadine as pH dropped, relative to amantadine-free monomer suspensions. That observation could help in understanding the pattern of amantadine block of proton transport shown here: amantadine enhancement of flux with declining experimental pH. Block patterns varied slightly from Set 1 to Set 2 of the liposome activation-saturation assays, and with proton flux capacity so radically reduced by increasingly acidic pH, efficacy of amantadine in blocking that flux was somewhat difficult to determine. It was clear, however, that amantadine did not prevent conductance of H^+ at low pH, and often served to increase proton flux above that in untreated M2(22-62) liposomes.

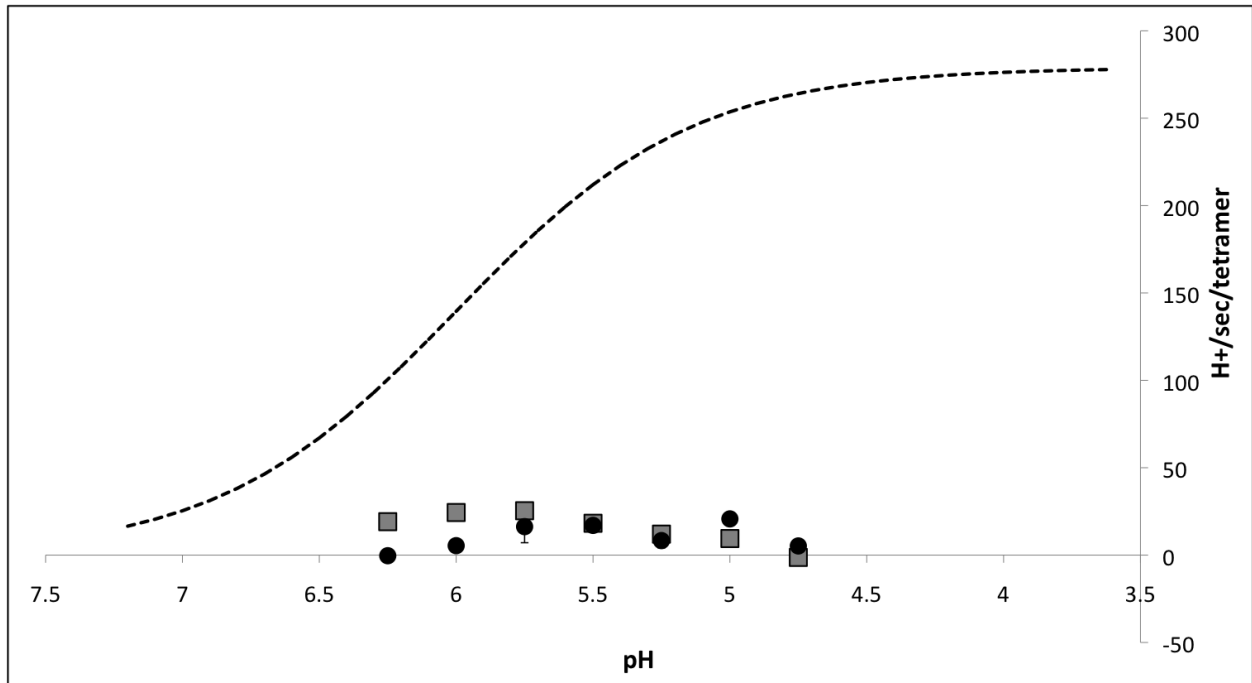


Figure 14.

Relation of Set 2 activation-saturation data to per-channel flux rates observed in *Xenopus* oocyte whole-cell voltage clamp assays. Dotted line represents a saturation curve with per-tetramer J_{\max} of 279 protons, and a pK of activation of 6.0. As in Fig. 8, gray squares indicate proteoliposome proton flux averages, and black circles indicate amantadine-incubated proteoliposome proton flux averages. Measurements were corrected for baseline H^+ leakage into the liposomes prior to valinomycin addition, and for valinomycin-induced H^+ leak observed in protein-free liposomes. Error bars are encompassed by the size of the markers.

M2(22-62) initial proton flux into buffer-saturated liposomes increased as external pH dropped from 6.5-5.5, indicating acid activation of the protein.

Proton flux measurements at experimental pH of 5.5 and above were higher here than in previous studies of M2 in liposomes due to a combination of factors. Some previous liposome assays^{26,27} used a valinomycin-induced membrane potential to drive proton flux, but no pH gradient from inside to outside the liposomes. Others⁵ included an extra-to-intra-liposomal pH difference of about 1 unit, but did not have a voltage gradient. The data presented here were gathered by utilizing at least 100-fold more $[H^+]$ outside the liposomes than in, and 100-fold

higher $[K^+]$ inside than out. Twice the driving force on the protons yielded higher flux rates than ever reported: up to 139 H^+ /tetramer/second, compared to a typical $<10 H^+$ /tetramer/second (at most 45 H^+ /tetramer/second²⁵) seen by others.

Additionally, the citrate buffer present in the extra-liposomal solution appeared to contribute to the high flux rates. Initial assay design employed very weakly-buffered external solution, but the extreme sensitivity of this solution composition to any addition of H^+ ions exacerbated the pre-valinomycin pH drift in the experiments, also making consistency and reproducibility difficult for series of experiments at identical pHs. Including citrate buffer in the external bath was a way to alleviate these difficulties, but was initially expected to also lower H^+ initial flux rates through M2(22-62) by binding available H^+ . The observed *increase* in flux with citrate-buffered external bath solution was unexpected, but upon further consideration it was decided that the buffer must actually have functioned as a free H^+ reservoir and delivery apparatus, bringing protons to the “depletion zone” created at the N-terminal side of the transporter as the protein transfers H^+ from outside the liposomes to inside⁸. Apparently, the citrate buffer is what helped to quickly and effectively deliver protons to the N-terminus of the channel/transporter, increasing the measured flux rates even further.

The observed loss of protein function at low pH could possibly be due, as mentioned above, to monomerization of M2(22-62) tetramers. A possible explanation for this phenomenon could be found in the same protonation of Histidine 37 that allows initiation of proton transport activity through the protein. Protonating the third His of the tetramer is the event which initiates H^+ flux³⁰, but forcing the external pH to low enough levels to add a fourth proton on the final His residue might actually cause electrostatic repulsion of each monomer in the tetrad, shifting M2(22-62) from a H^+ transporting state to an H^+ -desensitized state. If this were true, then a data

analysis model could present net proton transport activity as the product of the fraction of tetramers that are in the triply-protonated, actively conducting state and the fraction of tetramers that are over-protonated and desensitized, likely becoming monomerized. A chart was generated in Microsoft Excel, using the Solver add-in to computer-fit the entire data set (Set 1 data and Set 2 data) and project this net transport curve.

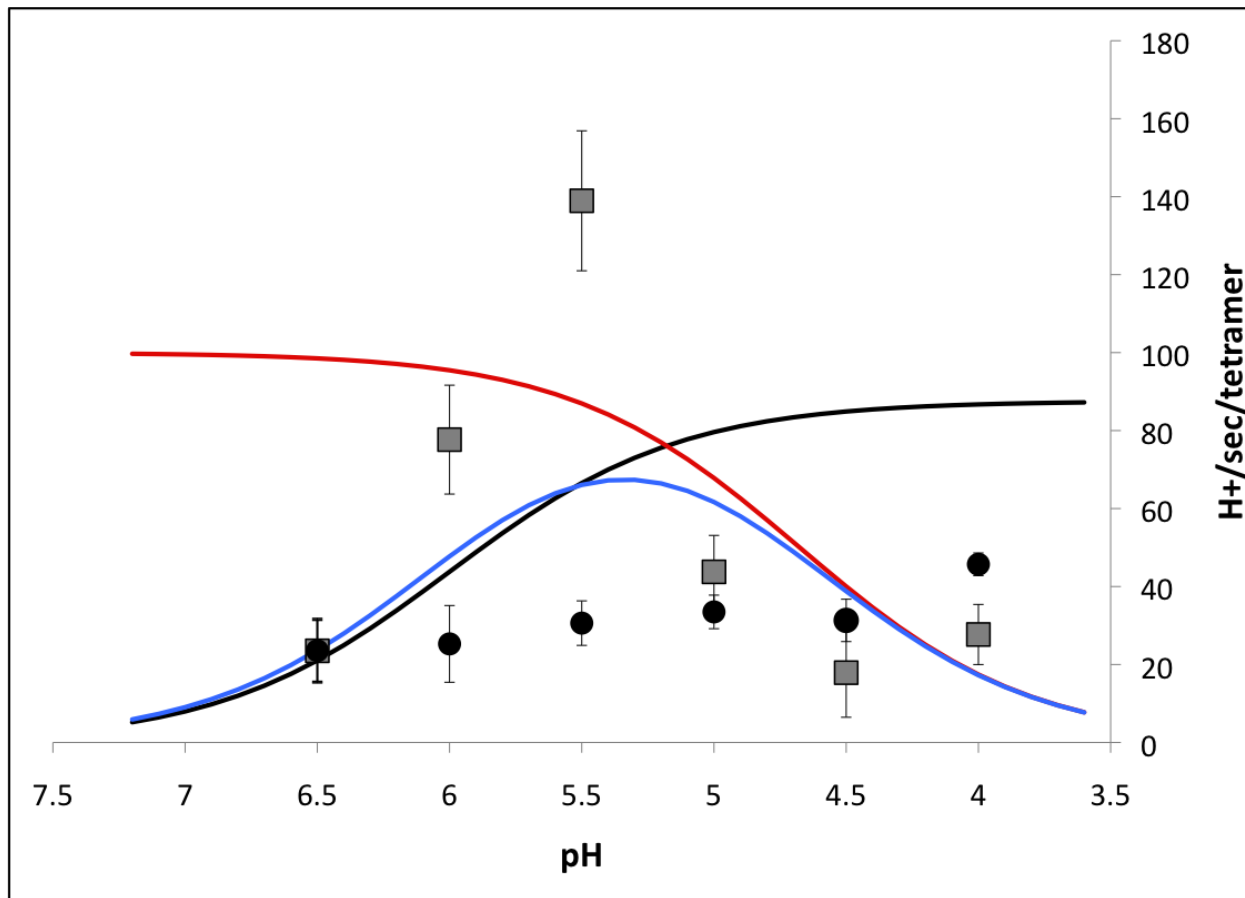


Figure 15.

Black curve=flux saturation with a set pK of 6.0¹ and a computer-fit J_{\max} of 87.6 H⁺/sec/tetramer. Red curve=protein loss of activity, with a set J_{\max} of 100 H⁺/sec/tetramer and a computer-generated pK of 4.7. Blue curve=net transport curve, the best fit to the data of a function of both saturation and inactivation curves.

Linking both data sets to each other, such that the J_{\max} of saturation and pK of inactivation of both were dependent on the saturation curve pKs being fixed at 6.0 (as justified

by the MEL cell study¹ and solid-state NMR-based mechanistic models^{23,30}) and both J_{\max} of inactivation being fixed at 100 H^+ /sec/tetramer. A net transport curve, dependent upon all data gathered, was generated for each individual data set.

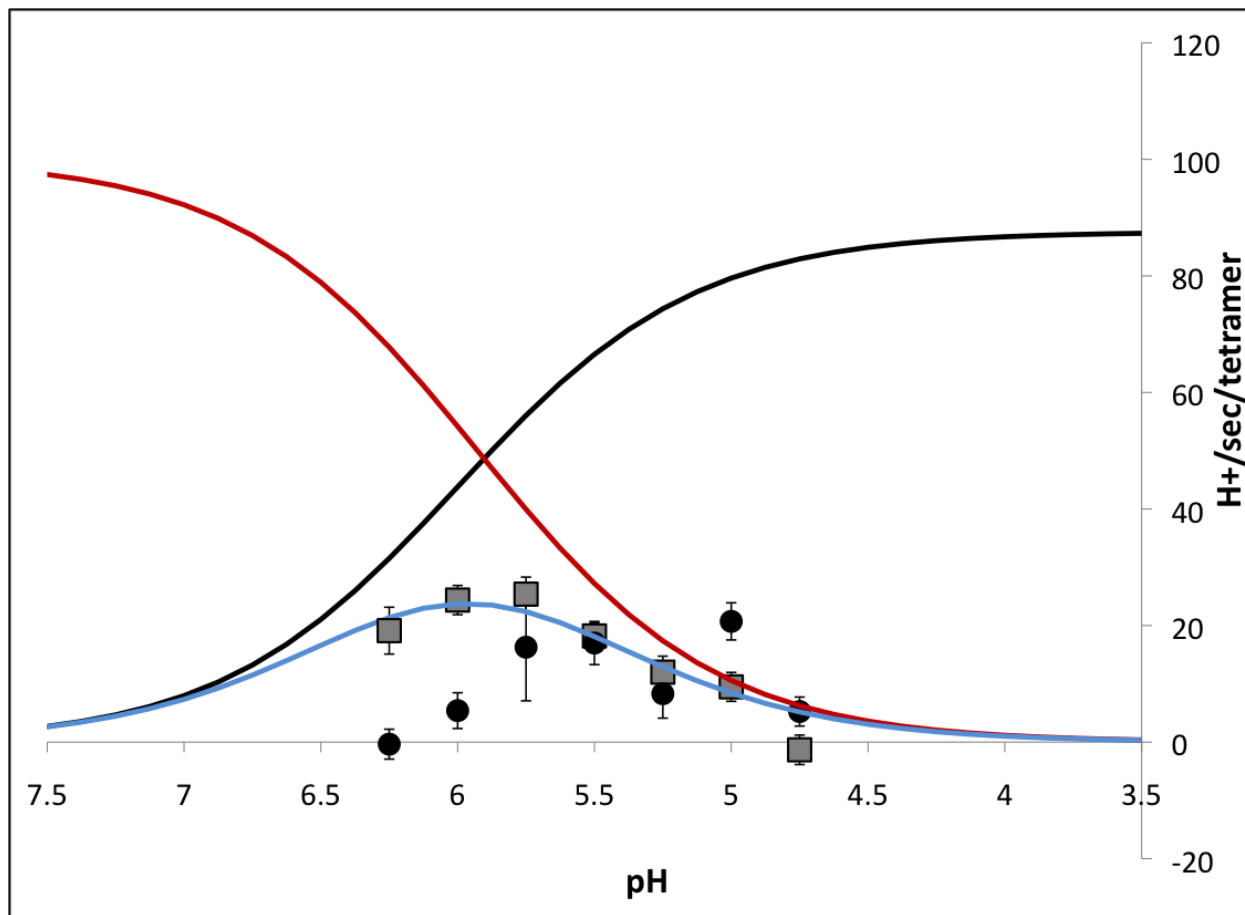


Figure 16.

Black curve=flux saturation with a set pK of 6.0¹ and a computer-fit J_{\max} of 87.6 H^+ /sec/tetramer. Red curve=protein loss of activity, with a set J_{\max} of 100 H^+ /sec/tetramer and a computer-generated pK of 5.9. Blue curve=net transport curve, the best fit to the data of a function of both saturation and inactivation curves.

This analysis indicated a saturation-inactivation pK of 4.7 in Set 1, but 5.9 in Set 2. Such heightened sensitivity of the peptide to acidic pH after long-term storage strengthens the claim that some form of peptide degradation, likely monomerization, occurred between the time when data Set 1 was gathered and data Set 2 was gathered. Future assays with M2(22-62) will likely

need to be completed within just a few months after peptide growth and purification, in order to avoid compromising data-gathering efforts, especially if low-pH experiments are planned.

The relationship between protein structure and function is a crucial element of the current efforts in the structural biology field to understand the M2 protein and generate new anti-influenza drugs. The functional assays performed have most often been intracellular electrophysiological assays, or now proteoliposome assays. But structural determination must be carried out in often extreme conditions, such as radically low temperatures for X-ray crystallography, stacked and compressed lipid bilayers for solid-state NMR spectroscopy, or heavy detergent concentrations for solution-state NMR. Native-like tetramerization of the protein is often difficult to achieve or determine, especially when using shorter constructs (M2 TMD, etc.) of the protein. The assumed structural changes M2 undergoes when transitioning from non-conducting to conducting states in response to external pH have also required studies to be carried out at an array of pHs, which can be logistically difficult. And, of course, the particular site of amantadine binding in a functionally blocked M2 tetramer is of critical interest to Influenza researchers.

The various structural approaches each have strengths and weaknesses, which has only made the discourse more heated as different approaches yield very different results in the attempts to elucidate M2 structure. Solution-state NMR of an M2(18-60) truncate with rimantidine in short-chain lipid/detergent (dihexanoyl phosphatidylcholine) micelles showed a nearly bilayer-perpendicular transmembrane helix, with rimantidine bound to the C-terminal, amphipathic helix at Asp 44 rather than the demonstrated primary amantadine-resistance residue, Ser 31. X-ray crystallography in octylglucoside of M2 TMD(25-45), however, showed amantadine interacting with residues 27-34, in the heart of a 35°-tilted (with respect to the

tetramer axis) tetramer³¹. Still another method, solid-state NMR, showed the M2(22-62) protein truncate in dioleoylphosphatidylcholine lipid bilayers having a transmembrane helix tilt angle of 32-22° (kinking at Gly 34), similar to the crystallographic finding, and the amphipathic helices splayed out at 105°, facing D44 toward the tetramer axis, rather than the lipid headgroups²³. Arguments of the validity of lipid vs. detergent environments, temperature constraints, most appropriate pH, etc. plague the structural biology discourse as researchers attempt to understand M2.

Reports on proposed structures claim to indisputably explain the mechanism of H⁺ flux through M2 (though a recent paper comparing structures determined at different pHs managed to reconcile a few disparate explanations into a dynamic model of proton movement²¹). But until functional assays can reliably validate their mechanistic models, it will be difficult to determine which version to trust when searching for, for instance, for amantadine alternatives. Elucidation of M2 H⁺ transport properties using an easily-quantified, well-controlled system like the proteoliposome proton flux assay is an essential step toward distinguishing which structural model(s) will be valuable in the search for new antiviral agents.

The functional data presented here significantly narrow the range of proposed structures to those few which can support a proton transport, not channel, model of the M2 protein. This implies a completely blocked pathway, interrupting any possible water wire. Definitive determination of transporter function through these highly robust liposome assays will give structural biologists an anchor from which to assess validity of proposed structural/mechanistic models. In addition, the acid-activation response of M2 flux was characterized by these data in a much more specific way than any previous studies, distinctly demonstrating an increase in H⁺ transport function from pH 6.5-5.5, and identifying the optimal transport pH in the narrow range

of 5.5-5.75. The observed amantadine effects on H^+ flux, evident in Set 2: loss of block capability as proton flux rates rose, then apparent stabilization of a blocked tetrameric form of M2(22-62)—possibly allowing proton flux around the drug in its binding site—will also be crucial in unequivocally identifying the exact mechanism of amantadine binding--the key to development of new anti-influenza pharmaceuticals.

APPENDIX

Optimal Liposome Protein Density Determination

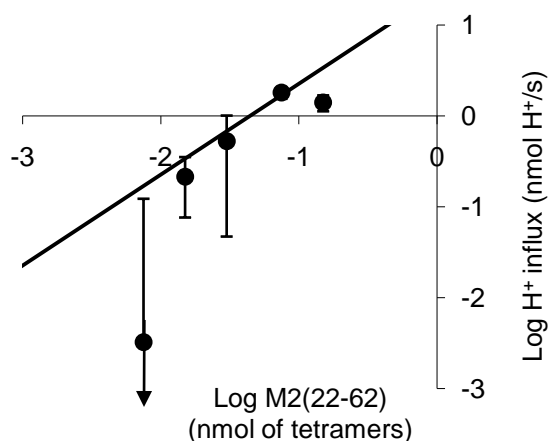


Figure 17.

To assess the oligomerization of M2(22-62), the proton transport rate as a function of protein density was measured. This figure shows the log of the initial liposomal proton uptake rate after valinomycin injection (H^+ /s) plotted against log of peptide content (nmoles of tetramer in the 3-ml assay). The theoretical line of unity slope shows the best fit of a line constrained to pass through the origin on a linear-linear plot, with slope of 23.8 H^+ /tetramer-s after protein orientation correction.

Optimal protein concentration was determined to be 0.1 mg protein:20 mg lipid by assaying proton flux into liposomes comprised of 0.05-0.2 mg protein:20 mg lipid and observing the highest flux rates at the 1:200 ratio.

Liposomal Lipid Quantitation/Verification

Quantification of liposomal lipid amount was necessary for determination of trapped volume, and to evaluate efficiency of the different extruders. A phosphate determination assay, based on that developed by Chen, Toribara, and Warner²⁴, was used to evaluate phospholipid amounts in purified lipid aliquots, unextruded lipid-protein suspensions, and suspensions passed through Avestin and Avanti extruders. Rather than using the typical internal liposome buffer, which contains phosphate and would confound the assay, liposomes were suspended in a buffer of 100 mM KCl, 10 mM HEPES buffer, pH 8.0. An array of PO₄ standards was assayed concurrently in order to generate a standard curve for phosphate quantity in the lipid or liposome samples. Briefly, the assay protocol consisted of: the lipid phase was extracted from the aqueous phase using methanol and chloroform. Organic solvents were evaporated with nitrogen gas, and 10% Mg(NO₃)₂•6 H₂O in ethanol was added. Mixture was evaporated/ashed over a flame until white. 1N HCl was added, solution vortexed, and then hydrolyzed in boiling water for 15 minutes. A solution of 1 part 10% ascorbic acid:6 parts molybdenum solution (1 part 6N H₂SO₄:2 parts H₂O:1 part 2.5% ammonium molybdate) was added and allowed to incubate for 20 minutes. Phospholipid concentration was proportional to OD at 820 nm. Unextruded liposome samples averaged 0.125 absorbance units, Avanti extruder samples averaged 0.120 absorbance units, and Avestin extruder samples averaged 0.145 absorbance units—obviously no lipid was *lost* from that extruder! These data indicated that little, if any, lipid was lost in extrusion with any of the equipment used.

Liposomal Protein Quantitation Attempts

Proteoliposome protein quantitation assays were not successful. Methods attempted included the BCA assay, purchased in a kit by Pierce from Thermo-Fisher Scientific, which utilized bicinchoninic acid to colorimetrically indicate protein quantity via UV absorbance at 562 nm. Protein control liposomes with bovine serum albumin were created, but were imperfect as reference proteoliposomes because of the inherent differences in liposome formation around a water-soluble protein versus a membrane protein. But the difficulty of isolating protein from lipid when assaying liposomes proved to be the confounding factor. Lipid interference was such that proteoliposomes and protein-free liposomes showed similar absorbance at 562 nm.

An acetone precipitation method was attempted, based on a “Tech Tip” included in the BCA assay documentation, to eliminate the contaminant lipid. The steps were: add 4x volume of cold acetone to protein standards and blanks, vortex and incubate 30 min at -20°C, centrifuge 10 minutes in a microcentrifuge at maximum speed, pour off supernatants and allow acetone to evaporate for 30 minutes at room temperature, then run BCA assay as above. M2(22-62) stock samples, suspended in methanol to a known protein concentration, were used as standards as well as BSA suspended in HEPES buffer. Methanol-suspended stock M2(22-62) was also diluted 1 part:2 parts water and spectroscopically analyzed for protein concentration before acetone precipitation, to be utilized as another standard. Unextruded, Avanti-extruded, Avestin-extruded, and protein-free liposomes were all assayed.

A nitric acid-based assay, based on the nitration of tyrosine residues in peptides, with resulting absorbance at 358 nm, was also attempted³². This assay was difficult and dangerous to perform, and the cuvettes used were melted and warped by the acid.

The Bradford assay using Coomassie Blue dye (or in this case, Sigma Brilliant Blue G-250—NOT “R”!), ethanol, and phosphoric acid as the colorimetric assay solution was the final attempt at protein quantitation in the liposomes. This assay allowed for low concentrations of certain detergents³³, including n-octylglucoside, which enabled detergent-solubilization of the liposomes to eliminate lipid contamination. 30% O.G. solution was used, then added to liposomes to a total concentration of 10% O.G. before reagent addition. Absorbance at 595 nm was to indicate total protein concentration, but results were confounding, as with the other assays attempted. It was at this point that the Leiding, et al²⁵ study was published, using a modification of a detergent-compatible commercial assay kit and demonstrating nearly 100% protein retention after liposome extrusion. In future studies, this method will be the assay of choice for liposome protein quantitation.

REFERENCES

Works Cited

1. Chizhmakov IV, Geraghty FM, Ogden DC, Hayhurst A, Antoniou M, Hay AJ. Selective proton permeability and pH regulation of the influenza virus M2 channel expressed in mouse erythroleukaemia cells. *J Physiol* 1996;494 (Pt 2):329-36.
2. Nayak DP BR, Yamada H, Zhou ZH, Barman S. Influenza virus morphogenesis and budding. *Virus Res* 2009;143:147-61.
3. Maugh TH. Amantadine: An Alternative for Prevention of Influenza. *Science* 1976;192:130-1.
4. Centers for Disease Control C. 2008-2009 Influenza Season Week 35 ending September 5, 2009. CDC website 2009; <http://www.cdc.gov/flu/weekly/weeklyarchives2008-2009/weekly35.htm>.
5. Pielak RM, Schnell JR, Chou JJ. Mechanism of drug inhibition and drug resistance of influenza A M2 channel. *Proc Natl Acad Sci U S A* 2009;106:7379–84.
6. Mould JA, Drury JE, Frings SM, et al. Permeation and activation of the M2 ion channel of influenza A virus. *J Biol Chem* 2000;275:31038-50.
7. Zhong Q, News DM, Pattnaik P, Lear JD, Klein ML. Two possible conducting states of the influenza A virus M2 ion channel. *FEBS Lett* 2000;473:195-8.
8. Busath D. Influenza A M2: Channel or Transporter? *Advances in Planar Lipid Bilayers and Liposomes* 2009;10:161-201.
9. Mould JA, Li H-C, Dudlak CS, et al. Mechanism for proton conduction of the M2 ion channel of influenza A virus. *J Biol Chem* 2000;275:8592-9.
10. Pinto LH, Holsinger LJ, Lamb RA. Influenza virus M2 protein has ion channel activity. *Cell* 1992;69:517-28.
11. Wang C, Lamb RA, Pinto LH. Activation of the M2 ion channel of influenza virus: a role for the transmembrane domain histidine residue. *Biophys J* 1995;69:1363-71.
12. Shimbo K, Brassard DL, Lamb RA, Pinto LH. Ion selectivity and activation of the M2 ion channel of influenza virus. *Biophys J* 1996;70:1335-46.
13. Wang C, Lamb RA, Pinto LH. Direct measurement of the influenza A virus M2 protein ion channel activity in mammalian cells. *Virology* 1994;205:133-40.
14. Chizhmakov IV, Ogden DC, Geraghty FM, et al. Differences in conductance of M2 proton channels of two influenza viruses at low and high pH. *J Physiol* 2003;546:427-38.
15. Hay AJ, Zambon MC, Wolstenholme AJ, Skehel JJ, Smith MH. Molecular basis of resistance of influenza A viruses to amantadine. *J Antimicrob Chemother* 1986;18 Suppl B:19-29.
16. Sharma M, Qin H, Peterson E, et al. Structural and Functional Studies of M2 Proton Channel from Influenza A Virus. In: 52nd Biophysical Society Meeting; 2009; Boston, MA: Biophysical Journal; 2009. p. 432a.
17. International Committee on Taxonomy of Viruses I. 00.046.0.01. Influenzavirus A. . ICTVdB - The Universal Virus Database, version 4 2006; <http://www.ncbi.nlm.nih.gov/ICTVdb/ICTVdb/00.046.0.01.htm>.
18. Tobler K, Kelly, M.L., Pinto, L.H. and Lamb, R.A. . Effects of Cytoplasmic tail truncations on the activity of the M2 ion channel of influenza A virus. . *J Virol* 1999;73:9695-701.

19. Ma C, Polishchuk AL, Ohigashi Y, et al. Identification of the functional core of the influenza A virus A/M2 proton-selective ion channel. *Proc Natl Acad Sci U S A* 2009;106:12283-8.
20. Peterson E, Ryser, T., Funk, S., Inouye, D., Sharma, M., Qin, H., Cross, T.A., Busath, D.D. Functional Reconstitution of Influenza A M2(22-62). *Biochimica et Biophysica Acta-- Biomembranes* 2010.
21. Acharya R, Carnevale V, Fiorin G, et al. Structure and mechanism of proton transport through the transmembrane tetrameric M2 protein bundle of the influenza A virus. *Proc Natl Acad Sci U S A* 2010;107:15075-80.
22. DeCoursey TE. Voltage-gated proton channels and other proton transfer pathways. *Physiol Rev* 2003;83:475-579.
23. Sharma M, Yi, M., Dong, H., Qin, H., Peterson, E., Busath, D.D., Zhou, H. Cross, T.A. Insight into the Mechanism of the Influenza A Proton Channel from a Structure in a Lipid Bilayer. *Science* 2010;330:509-12.
24. Chen T, Warner. Microdetermination of Phosphorus. *Journal of Analytical Chemistry* 1956;28:1756-8.
25. Leiding T, Wang J, Martinsson J, DeGrado WF, Arskold SP. Proton and cation transport activity of the M2 proton channel from influenza A virus. *Proc Natl Acad Sci U S A* 2010;107:15409-14.
26. Moffat JC, Vijayvergiya V, Gao PF, Cross TA, Woodbury DJ, Busath DD. Proton transport through influenza A virus M2 protein reconstituted in vesicles. *Biophys J* 2008;94:434-45.
27. Lin TI, Schroeder C. Definitive assignment of proton selectivity and attoampere unitary current to the M2 ion channel protein of influenza A virus. *J Virol* 2001;75:3647-56.
28. Wang J, Schnell JR, Chou JJ. Amantadine partition and localization in phospholipid membrane: a solution NMR study. *Biochem Biophys Res Commun* 2004;324:212-7.
29. Salom D, Hill BR, Lear JD, DeGrado WF. pH-dependent tetramerization and amantadine binding of the transmembrane helix of M2 from the influenza A virus. *Biochem* 2000;39:14160-70.
30. Hu J, Fu R, Nishimura K, et al. Histidines, heart of the hydrogen ion channel from influenza A virus: toward an understanding of conductance and proton selectivity. *Proc Natl Acad Sci U S A* 2006;103:6865-70.
31. Stouffer AL, Acharya R, Salom D, et al. Structural basis for the function and inhibition of an influenza virus proton channel. *Nature* 2008;451:596-9.
32. Scott A. Boerner, Yean K. Lee, Scott H. Kaufmann, Keith C. Bible. The Nitric Acid Method for Protein Estimation in Biological Samples. In: Walker JM, ed. *The Protein Protocols Handbook*. 2 ed: Humana Press Inc., Totowa, NJ:31-40.
33. Zuo S-S, and Per Lundahl. A Micro-Bradford Membrane Protein Assay. *Analytical Biochemistry* 2000;284:162-4.

CURRICULUM VITAE

Emily Peterson

463 E. Normandy Dr.
Provo, UT 84604

Phone: 801-471-7875
E-mail: epetey63@yahoo.com

Education

Brigham Young University Provo, UT

M.S.—Physiology & Developmental Biology – December, 2010

B.S.—Integrative Biology – April, 2006

Second major:—English

Research experience

Jan. 2009-Dec. 2010 BYU Physiology/Developmental Bio. Dept. Provo, UT

Thesis project: Electrophysiological analyses of transmembrane ion transport by Influenzavirus A M2 proton channel

- Proteoliposome proton flux assay development and execution; data analysis; peer-reviewed journal manuscript preparation and submission

Oct. 2007-Dec. 2008 BYU Physiology/Developmental Bio. Dept. Provo, UT

Part-time Faculty Research Associate

- Protein purification from bacterial cultures; use of various other molecular/cellular biology research techniques; use of planar bilayer analysis to study transmembrane proteins; experimental design; data analysis

Jan. 2004-July 2005 BYU Integrative Biology department Provo, UT

Aquatic Ecology lab/research assistant

- Participated in various lab research activities using field research techniques, microscopy, mass spectrometry, specimen identification of fish and aquatic macro- and microinvertebrates
- Planned, directed, executed faculty-mentored research project; supervised other undergraduates on that project and in care/maintenance of freshwater aquaria
- Sharma M, Yi, M., Dong, H., Qin, H., Peterson, E., Busath, D.D., Zhou, H. Cross, T.A. "Insight into the Mechanism of the Influenza A Proton Channel from a Structure in a Lipid Bilayer." *Science* 2010;330:509-12.
- Peterson E, Ryser, T., Funk, S., Inouye, D., Sharma, M., Qin, H., Cross, T.A., Busath, D.D. "Functional Reconstitution of Influenza A M2(22-62)." *Biochimica et Biophysica Acta--Biomembranes* 2010.
- "Acid-activation, Proton Transport Rate Saturation, and pH-dependence of Amantadine Block for Influenza A M2 Protein Truncate (22-62)." 53rd Biophysical Society Annual Meeting, San Francisco, CA. February 2010.
- "Functional Reconstitution of Influenza A M2(22-62)." 53rd Biophysical Society Annual Meeting, San Francisco, CA. February 2010.
- "Structural and Functional Studies of M2 Proton Channel from Influenza A Virus." 52nd Biophysical Society Annual Meeting, Boston, MA. Feb., 2009.
- Teaching Assistant/Student Instructor, Physiology 305 lab, BYU PDBio Dept., 3

Publications

Presentations

Scholarships/Awards

semesters (Winter & Fall 2009, Fall 2010).

- Research Assistantship, BYU PDBio Dept., Winter Semester 2010.
- BYU Women's Research Institute Travel Award, Winter Semester 2009.
- BYU Graduate Student Society Research Presentation Award, Winter Semester 2009.